NASA CR-66155

ANALYTICAL AND EXPERIMENTAL STUDY OF ALTITUDE COMPENSATION OF A ROCKET BY SECONDARY INJECTION

JUNE 1966

Prepared under Contract No. NAS 1-4102, Phase II by
Research and Development Department
Vickers Incorporated Division
Sperry Rand Corporation
Troy, Michigan 48084

LANGLEY RESEARCH CENTER

NATIONAL AERONAUTICS AND SPACE ADMINISTRATION

STUDY OF PROPORTIONAL SOLID PROPELLANT SECONDARY INJECTION THRUST VECTOR CONTROL UNDER SIMULATED ALTITUDE CONDITIONS

JUNE 1966

Prepared under Contract No. NAS 1-4102, Phase I by
Research and Development Department
Vickers Incorporated Division
Sperry Rand Corporation
Troy, Michigan 48084

LANGLEY RESEARCH CENTER

NATIONAL AERONAUTICS AND SPACE ADMINISTRATION

ABSTRACT

The object of this study was to obtain a better insight into the mixing effects associated with supersonic injection into a supersonic main stream and also explore the feasibility of altitude compensation and thrust augmentation of an altitude rocket motor. This program was instigated as an off shoot of contracts NAS 1-2962 and Phase 1 of NAS 1-4102 which investigated TVC by gaseous secondary injection of 2000°F gas under sea-level and altitude conditions.

For this study a secondary gas flow was injected into the 37.5:1 area ratio nozzle of a sub-scale rocket motor. Both the primary and secondary gases were at a nominal temperature of 2000°F.

A theoretical model of the phenomenon was developed and two experimental evaluations were carried out under sea-level conditions; the first utilizing 4 injection ports and the second 6 ports. During the second test the flow of injected gas was modulated to determine the effects of varying the injected to primary flow ratio.

The amount of nozzle pressure compensation and axial thrust augmentation was measured and compared to the theoretical predicted values.

FOREWORD

This report describes the results of work accomplished under Phase II of NASA Contract NAS 1-4102, entitled "Secondary Injection Thrust Vector Control for High Altitude Nozzles".

The contract was performed under the technical cognizance of Mr. John Riebe, Langley Research Center.

TABLE OF CONTENTS

TABLE OF CONTENTS
(Continued)

TABLE OF CONTENTS
(Continued)

LIST OF FIGURES

LIST OF FIGURES
(Continued)

LIST OF TABLES

NOMENCLATURE

Symbol	Definition	Units
A	Area	sq. in.
C	Loss Factors	
C_D	Discharge Coefficient	
D	Diameter	inches
h	Accomodation Height	inches
L	Distance from Nozzle Exit	inches
L_x	Distance from Port to Shock	inches
M	Mach Number	
P	Pressure	psia
P_2	Shock Pressure	psia
$\overline{P}_2$	Average Shock Pressure	psia
$\overline{P}_s$	Average Pressure in Separated Region	psia
R	Gas Constant	ft lb/lbm $^\circ$R
r	Radius	inches
r_b	Blend Radius	inches
T	Temperature	$^\circ$R
w	Weight Flow	lb/sec
X	Number of Injectors	
α	Half-Cone Angle	degrees
Γ	Thrust	pounds
γ	Specific Heat Ratio	
δ	Separation Angle	degrees
θ	Shock Angle	degrees

SUBSCRIPTS

Symbol	Definition
a	Ambient
c	Nozzle Chamber
e	Nozzle Exit
j	Injection Nozzle
o	Plane Containing Shock Apex
s	Separation Region
t	Total
3	Main Flow Conditions at Rocket Exit
4	Secondary Flow Conditions at Rocket Exit
*	Nozzle Throat

SECTION 1

INTRODUCTION

Contracts NAS 1-2962 and NAS 1-4102 covered the study of thrust vector control by the injection of warm gas (2000°F) into the nozzle extension cone of a high energy solid propellant (6200°F) rocket motor. In the initial contract (NAS 1-2962) tests were conducted under sea-level conditions using an 8:1 area ratio nozzle and in the second contract (NAS 1-4102) the same motor and injection system were tested under simulated altitude conditions using a rocket motor nozzle area ratio of 37.5:1.

During this program it was decided to investigate on a subscale motor the effects of secondary injection of higher mass flow ratios on the axial thrust of an altitude nozzle operating under sea-level conditions. If a significant amount of axial thrust augmentation could be achieved economically by compensating the altitude nozzle at sea level, then this approach could be used in designing a one stage to orbit booster. The amount of injected gas would be decreased as the vehicle gained altitude, so that the nozzle would operate near its optimum design point at all altitudes. Part of the injected gas would also be used for thrust vector control by differential secondary injection in the desired control plane.

The program plan detailed below was designed to obtain preliminary data on the feasibility of this concept.

1.1 Program Plan

The program was conducted according to the following plan:

1. Prepare an analytical model of the phenomenon with four port secondary injection.

2. Conduct an experimental evaluation in a sea level environment using a subscale motor mounted in a thrust measuring stand.

3. Analyze the test data from the firing and compare the results to the analytical model.

4. Based on the results of test 1 prepare an analytical model for 6 port injection.

5. Conduct an experimental evaluation of 6 port injection with modulated secondary injected flow.

6. Compare the test results with the analytical model.

SECTION 2

TEST PROGRAM

The test program consisted of two firings using a subscale rocket motor mounted on an axial thrust stand.

The following subsections describe the motor and instrumentation used to carry out the experimental phase of the program.

A sketch of the setup for the first test is shown in Figure 2.1.

2.1 Subscale Rocket Motor and Injection System

The rocket motor consisted of a heavyweight gas generator, a 37.5:1 area ratio nozzle and associated manifolding. The gas generator was loaded with a solid propellant grain which produced 0.58 lbs/sec of gas at 2000°F. The nozzle throat was sized to obtain a chamber pressure of 1000 psia.

The injection system consisted of a gas generator of the same capacity as the rocket motor. The gas from this generator was manifolded directly into the nozzle exit cone of the motor for the first test.

For the second test the gas was ported through a proportional high temperature pneumatic control valve, which modulated the

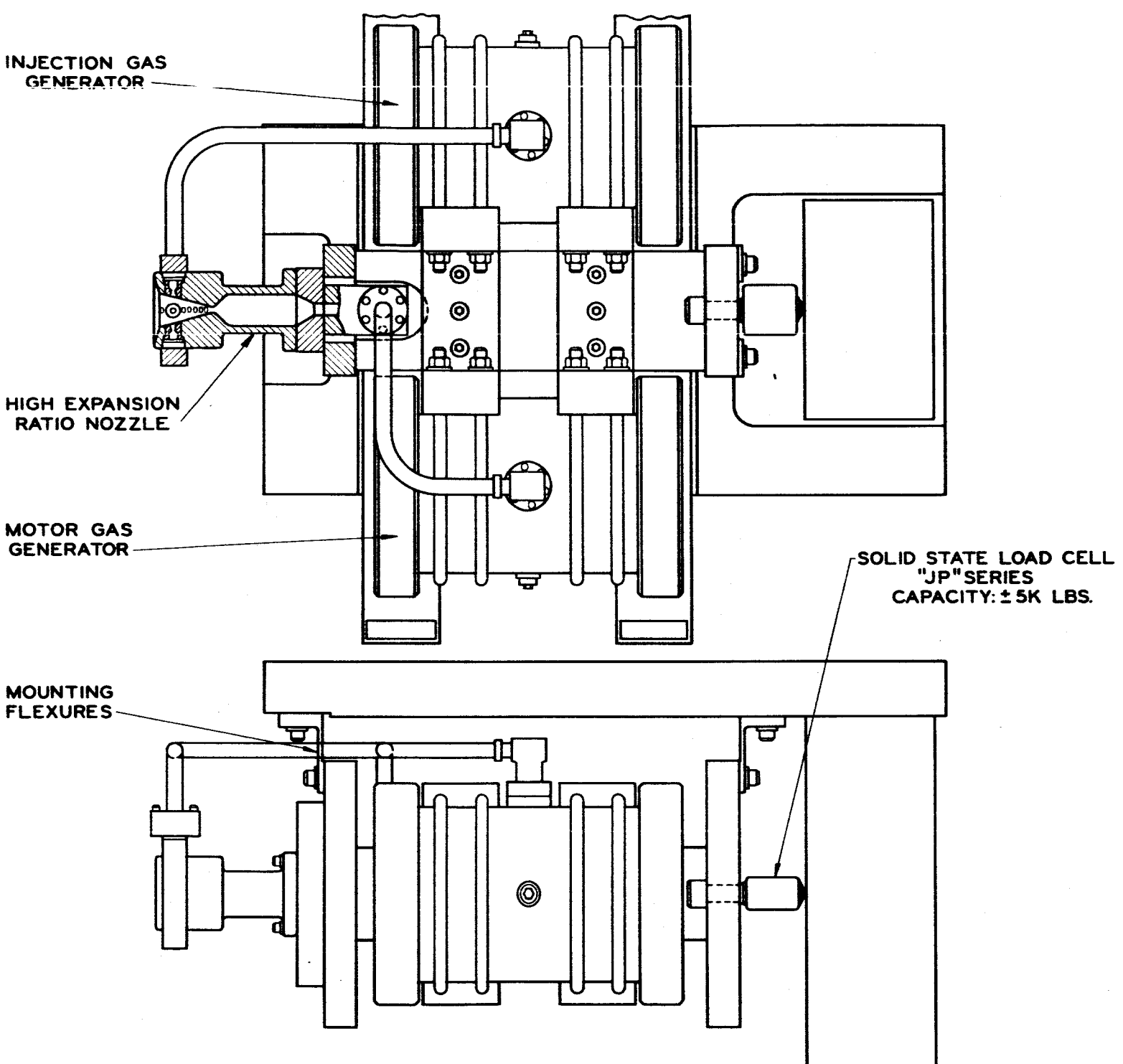

FIGURE 2.1 INSTALLATION OF MOTOR AND INJECTION SYSTEM ON THRUST STAND, TEST NO. 1

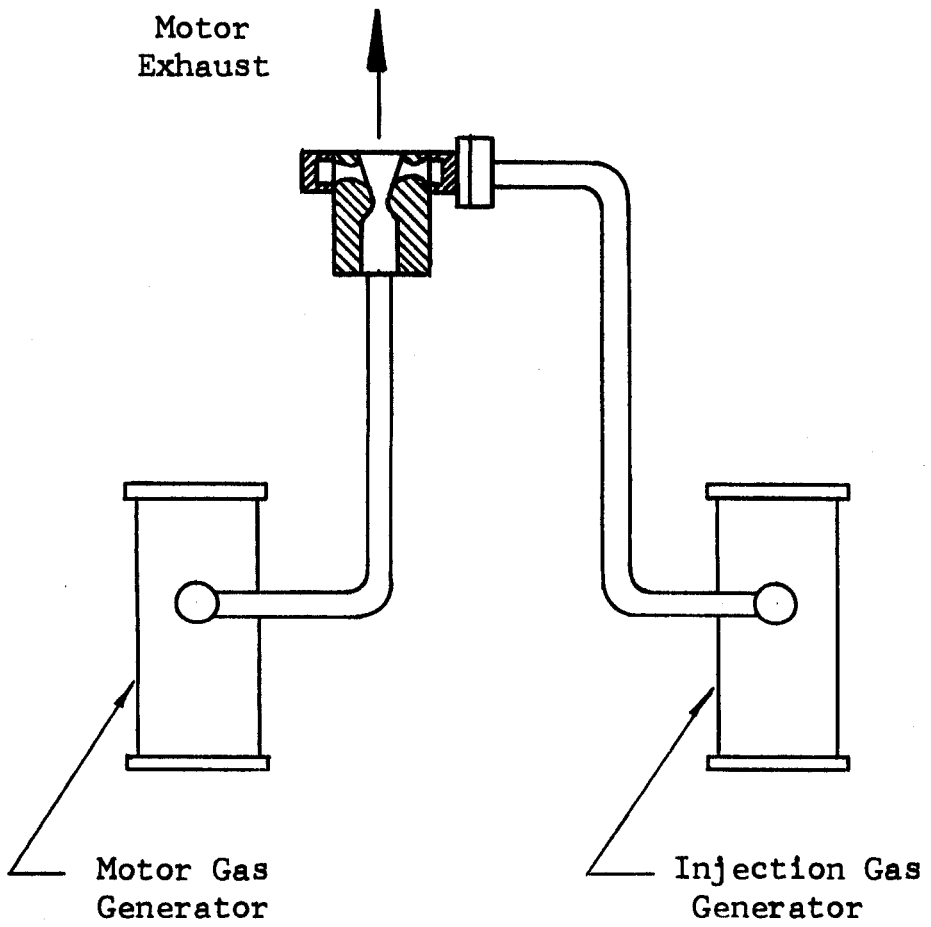

a. Test No. 1

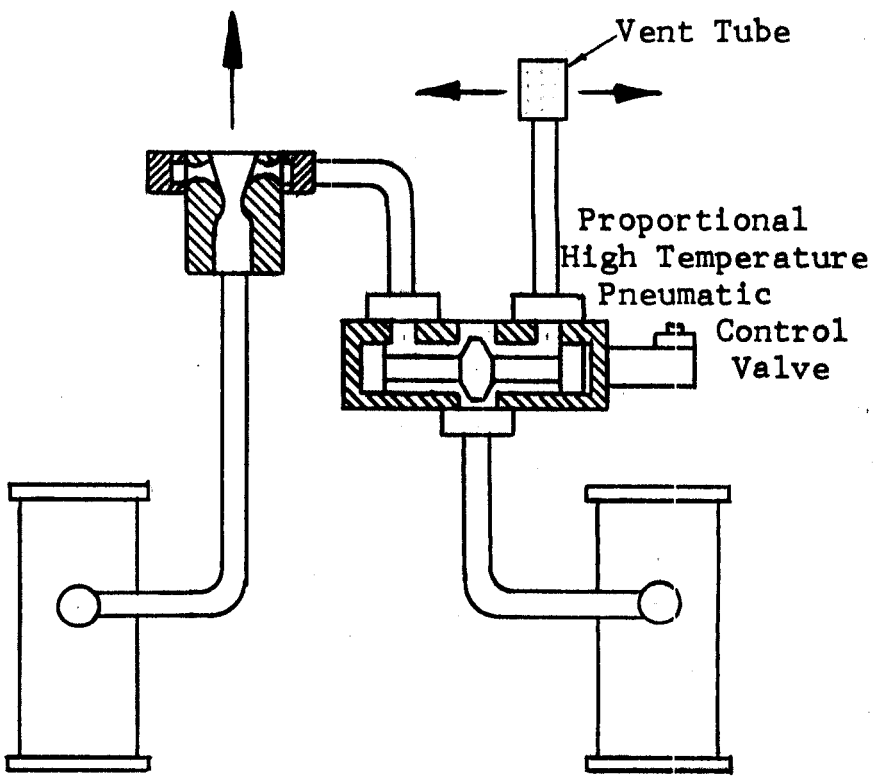

b. Test No. 2

FIGURE 2.2 SYSTEM SCHEMATIC

amount of injected gas in response to a programmed input signal. The design parameters for the motor and injection system for each test are given in Sections 3 and 4.

Eight pressure taps were machined into the nozzle exit cone to record static pressure levels during the tests. The location of these for each test are detailed in Sections 3 and 4. The complete system is shown in Figure 2.2.

Figure 2.3 is a photograph of the set-up taken during the second test firing.

2.2 Instrumentation

The following parameters were recorded during the two test firings.

1. Axial thrust.
2. Motor chamber pressure.
3. Injection nozzle chamber pressure. (This was measured in the annulus that supplied the multiple injection ports).
4. Gas temperature - motor chamber.
5. Gas temperature - injection annulus.
6. Eight (8) static pressures in the motor nozzle exhaust cone.
7. Gas generator pressure - motor.
8. Gas generator pressure - injection system.

In addition, for the second test in which the injected flow was modulated by a control valve, the valve input signal and valve position were also recorded. A slow double ramp input signal was fed into the control valve to modulate the injected flow from full to zero and back to full over a period of approximately 15 seconds.

SECTION 3

TEST RESULTS

TEST NO. 1 - FOUR INJECTION PORTS WITH CONSTANT INJECTED FLOW

3.1 Nozzle Dimensions

The dimensions of the 37.5:1 altitude nozzle, position of the injection nozzles and the location of the static pressure taps are shown in Figure 3.1.

3.1.1 Area Ratio Versus Axial Distance From Throat

Based on the blend radius (.300 inches) at the throat of the primary nozzle, the horizontal distance from the throat (x) corresponding to a particular area ratio is determined from the following equation:

$$x = .5607 \left[\sqrt{\frac{A}{A^*}} - 1 \right] + 0.040$$

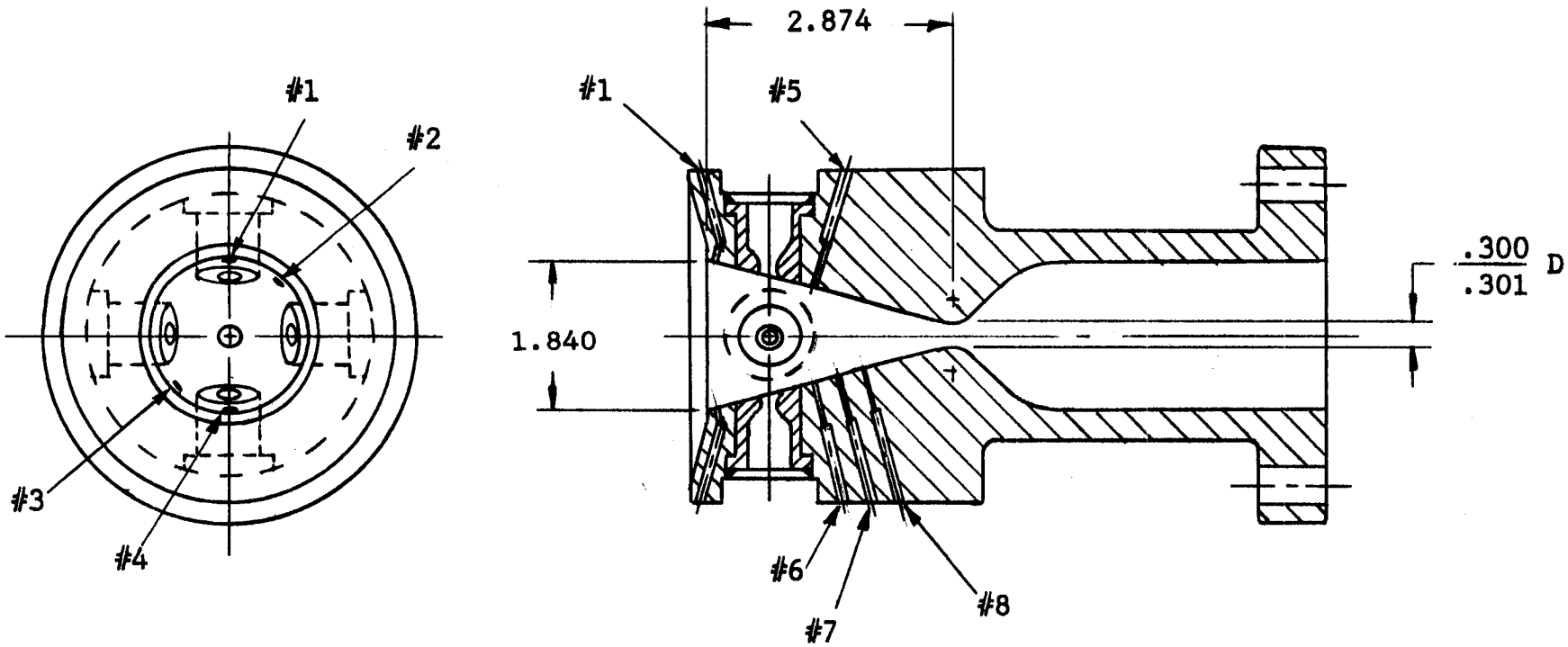

FIGURE 3.1 STATIC TAP LOCATIONS

3.1.2 Static Pressure Measurements

The nominal horizontal locations of the pressure taps from the throat are:

#8 - 1.129 in.

#7 - 1.441 in.

#5 & #6 - 1.753 in.

#1 thru #4 - 2.822 in.

Pressures were recorded at these taps throughout the firing. Table 3.1, Figures 3.2 and 3.3 contain samples of these pressure measurements. They were checked for correlation with the theoretical pressure distribution, corrected for horizontal position at a recorded primary chamber pressure of 925 psia (10 seconds). Figure 3.4 is the plot of this data. It can be seen that the theoretical and actual pressure distributions agree very closely until separation occurs within the nozzle.

Separation apparently occurred near 4 psia, which was the lowest recorded pressure within the nozzle. This agrees very well with an assumed theoretical pressure at which separation could take place $-0.283\ P_{amb} = 4.04$ psia.

TABLE 3.1

PRESSURE TAP MEASUREMENTS

	Time (Sec)	#1 (PSIG)	#2 (PSIG)	#3 (PSIG)	#4 (PSIG)	#5 (PSIG)	#6 (PSIG)	#7 (PSIG)	#8 (PSIG)
Primary Nozzle Only	0	0	0	0	0	0	0	0	0
	5	-0.6	-0.7	-0.7	-0.6	-10.4	-13.2	-8.0	-4.0
	10	-0.7	-0.6	-0.7	-0.6	-10.4	-10.4	-7.2	-4.0
Primary and Injector	12	+2.6	+1.7	+1.6	+2.8	+16.8	+16.4	+16.4	-3.8
	15	+2.6	+1.7	+1.6	+3.2	+20.8	+20.0	+20.0	-0.8
	20	+5.4	+2.1	+1.6	+5.0	+23.0	+23.6	+22.4	+15.6
	25	+3.9	+0.2	+2.2	+4.2	+24.8	+25.2	+23.4	+24.0
	30	+3.6	+0.2	+2.2	+4.2	+24.8	+25.4	+24.6	+24.4
	35	+4.4	+0.6	+3.6	+4.5	+22.8	+22.4	+22.0	+20.8
	40	+4.6	+2.9	+2.0	+4.9	+22.8	+22.8	+23.0	+20.0
	45	+5.2	+3.2	+2.0	+5.6	+23.0	+23.6	+24.6	+21.8
	50	+5.2	+3.0	+2.0	+4.9	+25.0	+25.8	+26.4	+24.0
	55	+4.8	+1.1	+1.7	+4.8	+26.4	+26.4	+28.0	+25.2
Injector Only	57.5	-1.7	-4.5	-4.0	-0.8	+41.8	+41.0	+37.2	+36.0
	60	-2.1	-4.0	-3.2	-1.0	+30.8	+30.2	+40.4	+43.6
	65	-1.8	-2.4	-2.0	-1.4	+17.0	+17.0	+23.2	+26.4
	68.5	0	0	0	0	0	0	0	0

Barometric Pressure 29.16 in. Hg
14.32 psi

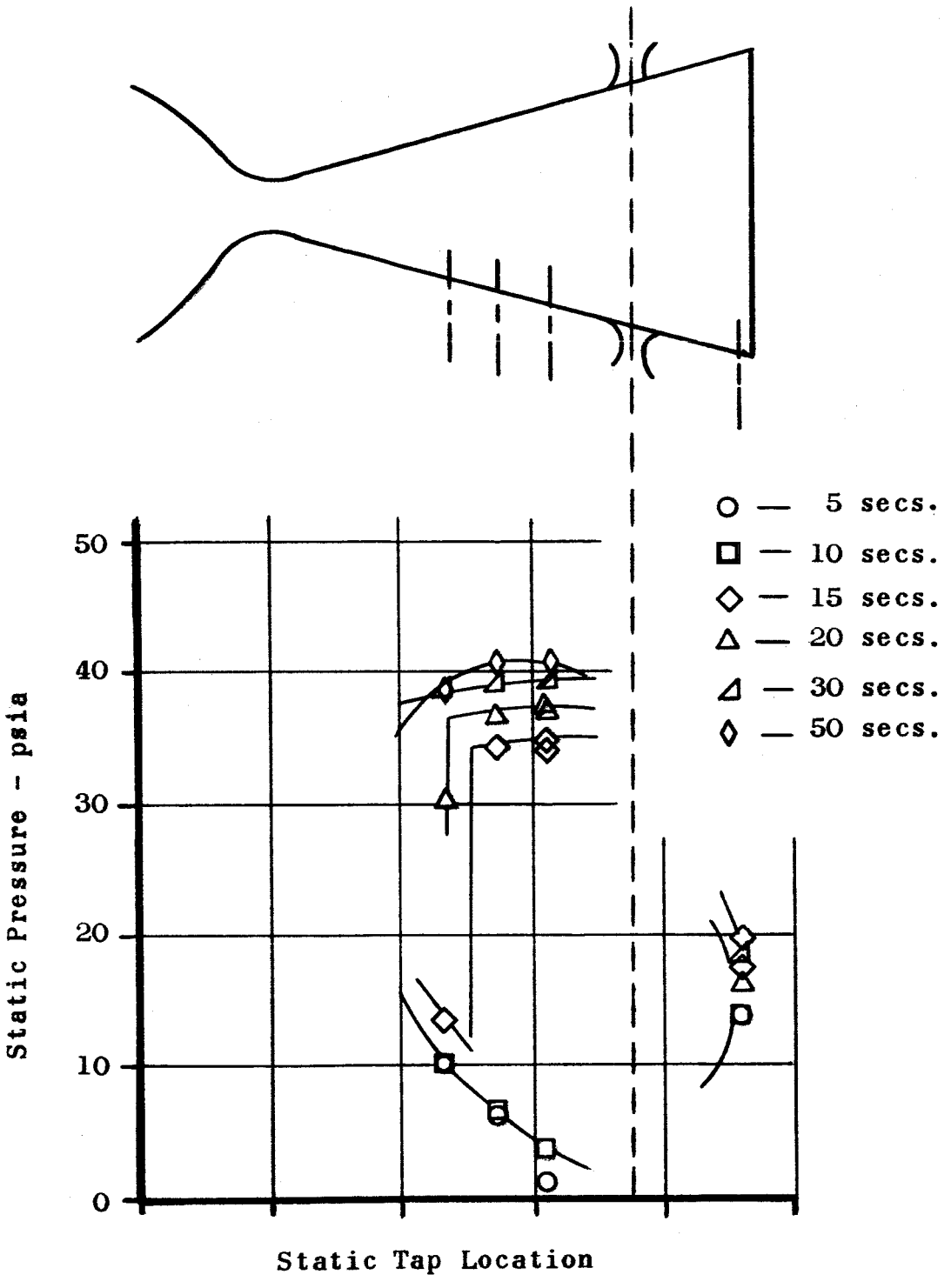

FIGURE 3.2 STATIC PRESSURE DISTRIBUTION WITHIN THE PRIMARY NOZZLE

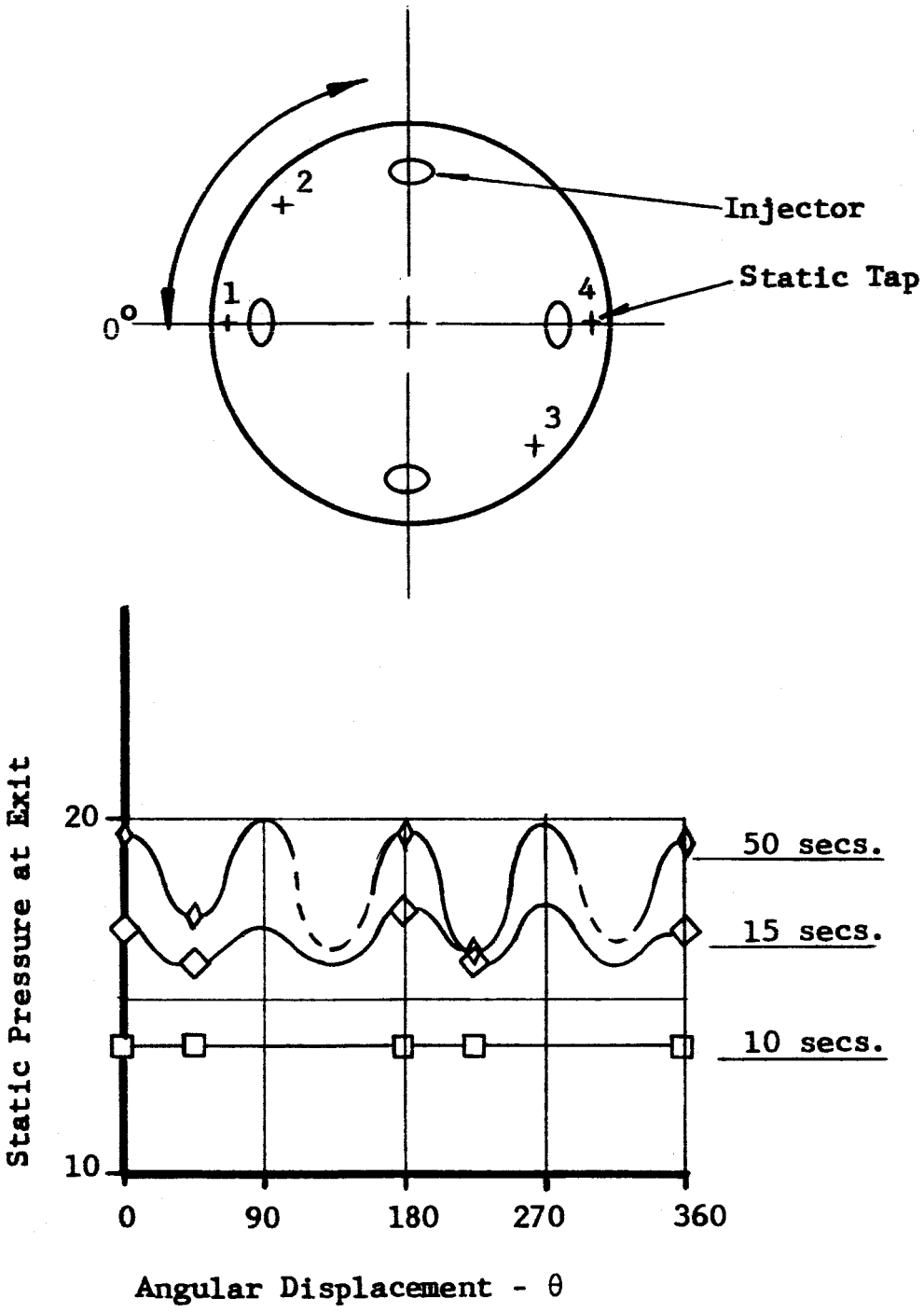

FIGURE 3.3 PERIPHERAL DISTRIBUTION OF STATIC PRESSURES AT EXIT OF PRIMARY NOZZLE

FIGURE 3.4 COMPARISON OF THEORETICAL AND MEASURED STATIC PRESSURES BEFORE AND AFTER SECONDARY INJECTION

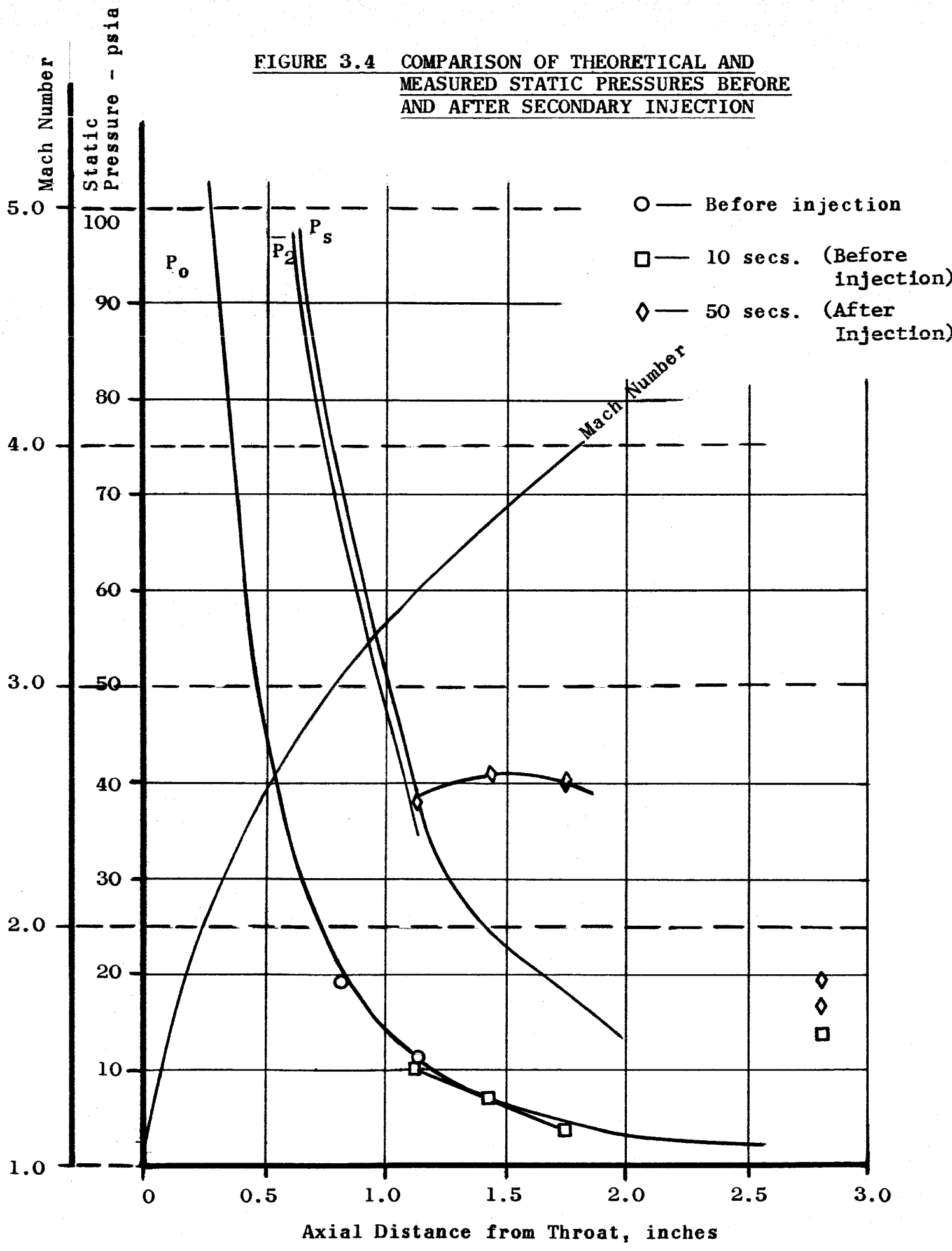

After the secondary generator was ignited, the pressure within the primary nozzle upstream of the injectors increased from 10.3 psia (10 sec.) to approximately 38.3 psia (50 sec.) at the location of tap #8, closest to the throat. The trend with time of the pressure measurement at tap #8 indicated that the steady state shock apex was situated very close to the tap's location. The separation pressure, P_s, based on the calculated Mach number, is 39.0, which compares very favorably with the measured pressure. These values are also plotted in Figure 3.4.

The pressure at the exit taps (1-4) was increased to a measurement between 1-5 psi above ambient pressure (Figure 3.3). The pressure between the injectors was slightly lower than that in line with the injectors. This circumferential distribution was improved with the use of 6 injectors (Section 4).

3.1.3 Thrust Measurements

The maximum primary thrust was 92.5 pounds and the maximum combined thrust was 139 pounds, which was a 50 percent increase in the thrust due to secondary injection. The thrust measurements variation with time are plotted on Figure 3.5.

FIGURE 3.5 THRUST MEASUREMENTS

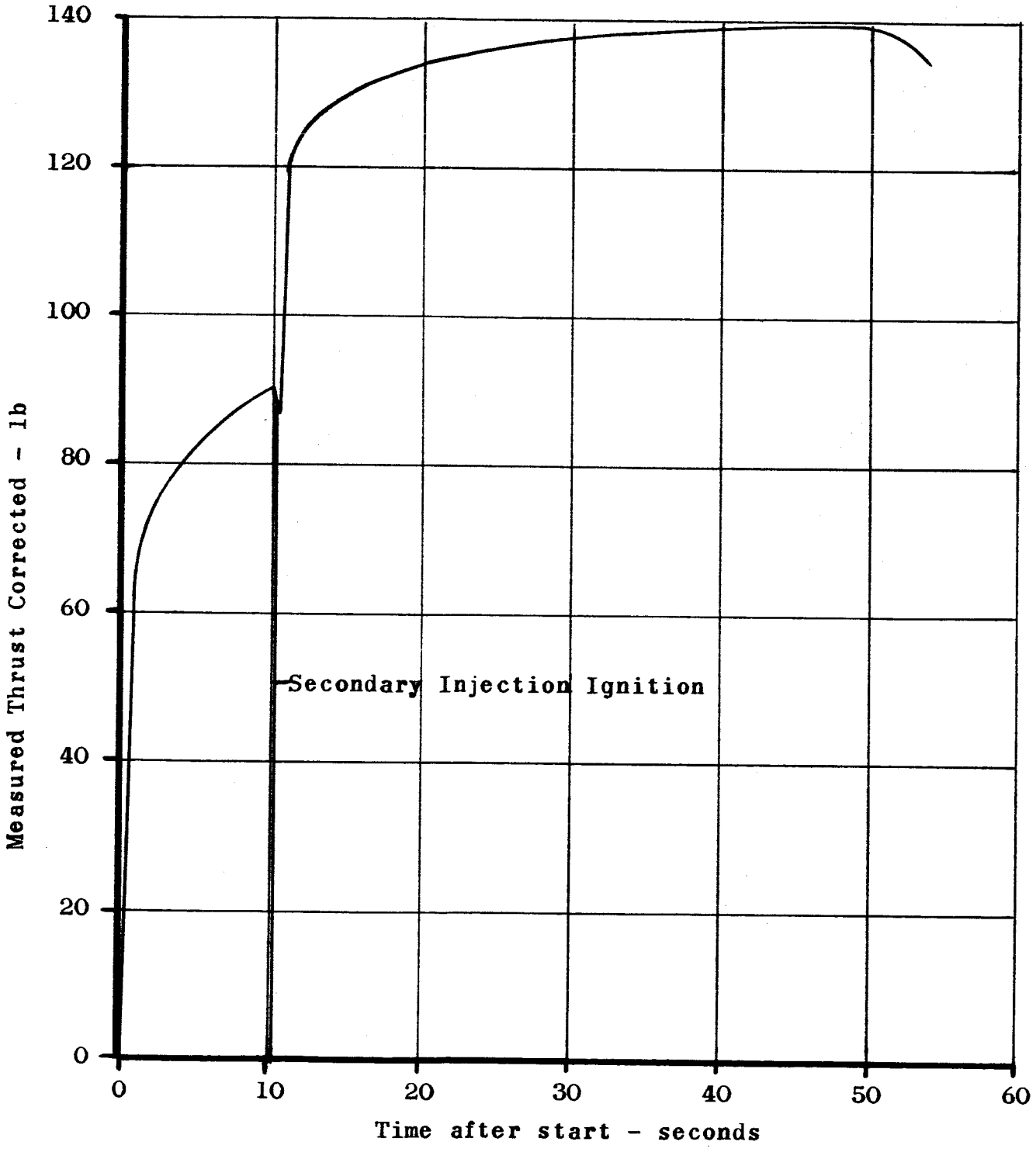

3.2 Correlation with the Analytical Model for Supersonic Injection into Supersonic Mainstream

Table 3.2 is a summary of the propellant properties recorded at t = 50 seconds.

	Primary Nozzles	Injector System
Weight Flow (lb/sec), w	0.565	0.565
Nozzle Chamber Pressure (psia), P_c	1005	935
Nozzle Total Pressure After Shock, P_{t_3}	850	
Separation Pressure = Secondary Total Pressure (psia), $P_s = P_{t_4}$		38.3
Exit Pressure (psia), P_3	16.8	
Exit Pressure (psia), P_4	19.3	
Nozzle Chamber Temperature (^oR) T_c	2370	2240
Ratio of Specific Heats, γ	1.279	1.279
Gas Constant ft lb/lbm ^oR	80.3	80.3

TABLE 3.2

RECORDED PROPERTIES - 50 SECONDS AFTER PRIMARY IGNITION

3.2.1 Calculation of Exit Area Based on Adjusted Value of P_{3_t} and P_{4_t}

The shock apex location was determined at pressure tap #8 in Section 3.1.2. Tap #8 is a nominal 1.129 inches from the throat which is 1.066 inches horizontally upstream of the injector location. This position corresponds to a $M_o = 3.39$ (see Figure 3.4). Based on data obtained from the firing it has already been stated in Section 3.1.2 that the actual and theoretical separation pressures agree very favorably, 38.3 to 39.1 psia. Therefore, it was felt that the separation angle, σ, presented in Mager's papers (References 2 and 4) were also accurate. The separation angle, σ, corresponding to $M_o = 3.39$ is 20.4°.

The total pressure loss across the shock can be approximated as 15 percent from Reference 5 for the separation angle and Mach number values obtained. Therefore, the total pressure of the primary stream after the shock is now 850 psia rather than 1005 psia at 50 seconds.

In the analysis and design of the nozzle, it was assumed that little or none of the dynamic head of the secondary injectant will be recovered so that the total pressure of the secondary stream at the nozzle exit was equal to the upstream separation pressure. Thus, the value of P_{t_4} was taken to be 38.3 psia.

The exit pressure measured at taps 1 thru 4 indicates 19.3 psia in line with the injectors, and 16.8 psia between them. The 16.8 psia exit pressure was taken as P_3 and 19.3 psia as P_4.

The area at the exit tap is $A_3 + A_{4_{total}}$. A summary of these calculated values is contained in Table 3.3. The geometrical area available at the location of the exit pressure taps is 2.459 in^2. From Table 3.3 the area calculated was 2.165 in^2, or the calculated area is 12 percent smaller than the actual area.

3.2.2 Thrust Based on the Calculated Area

Assuming no mixing, the thrust based on the calculated areas was determined by the basic thrust equations rearranged in terms of the exit conditions:

$$\Gamma_3 = A_3 \left[0.983 M_3^2 \gamma P_3 + (P_3 - P_{amb})\right]$$

$$\Gamma_4 = A_4 \left[0.983 M_4^2 \gamma P_4 + (P_4 - P_{amb})\right]$$

0.983 is the divergence coefficient, λ, a function of the divergence half angle, 15°, of the nozzle.

The thrust contribution from the primary flow was calculated to be 99.4 pounds and from the secondary flow 54.9 pounds for a total axial thrust of 154.3 pounds, which is approximately 11 percent higher than the measured value.

TABLE 3.3

CALCULATED FLOW PERFORMANCE OF FOUR INJECTION DESIGN

P_{t_3}			850 psi
P_3			16.8 psia
M_3			3.115
A_3			0.480 in^2
P_{t_4}			38.3 psia
P_4			19.3 psia
M_4			1.068
$A_{4_{total}}$			1.685 in^2
$A_e=A_3+A_{4_{total}}$	0.480+1.685	=	2.165 in^2
T_3			99.4 lbs.
T_4			54.9 lbs.
Γ_{total}	99.4+54.9	=	154.3 lbs.
Γ_{meas}			139 lbs.
λ			0.983
L_x (calculated)			1.542 inches
L_x (act.)			1.066 inches
h (calculated)			0.518 inches
h (corr.) = 0.72h (calculated)			0.373 inches

3.2.3 Evaluation of the Theoretical Accomodation Height at the Injector

Dividing $A_{4_{total}}$ by the number of injectors (4) determines the contribution of one injector to the area of the primary nozzle. The flow was assumed to take a hemi-cylindrical shape and the accomodation height, h, can be solved from geometry:

$$h = \left[\frac{2A_{4_{total}}}{4\pi}\right] = .518 \text{ inches}$$

The calculated distance from the apex of the shock to the center of the injection port (perpendicular injection) depends on the separation angle and the accomodation height:

$$L_x = h\ (\cot \delta + \tan \alpha) = 1.524 \text{ inches}$$

$$\delta = 20.4°$$

$$\alpha = 15°$$

$$h = 0.518 \text{ inches}$$

This distance parallel with the primary nozzle centerline is:

$$L_x \cos \alpha = 1.472 \text{ inches}$$

It was reported at the beginning of this paragraph that the distance from the injector port to the shock apex was 1.066 inches. Therefore, the actual to theoretical ratio is 72 percent. Based on the reasonable assumption that since the actual and theoretical separation pressures agree, the separation angle also agrees; the accomodation height at the injection

port can be corrected to 0.72h (calculated) for future preliminary designs. However, the accomodation height at the exit tap remains its theoretical value.

3.2.4 Estimated Mixing Losses Between Primary & Secondary Flows

Because the shock location was not the same as had been assumed in the design, the pressures behind the shock were also lower than had been assumed and therefore, the area ratio of the injector was mismatched to the existing exit condition; i.e., the flow in the injector was under-expanded when it exited into the primary nozzle. The design exit pressure of the injector was 80 psia, whereas the separation pressure was measured as 38.3 psia. It is felt that this mismatch may have led to excessive mixing losses and contributed to the lower than predicted thrust level.

A calculated thrust level and area ratio were determined from experimental values of static pressure measured during the test firing. These values are plotted as the intersection point of $C_3 = 1.00$ and $C_4 = 1.00$ lines in Figure 3.6. A family of curves of area and thrust for C_3 varying from 0.10 to 1.00 and C_4 varying from 1.00 to 1.4 are also plotted in Figure 3.6.

The intersection point of the actual area and the measured thrust occurs for $C_3 \triangleq .20$ and $C_4 \triangleq 1.07$; that is the correlation of the calculated and actual values of thrust and area occurs with a primary nozzle total pressure loss of approximately 80% and a secondary stream total pressure increase of 7%.

Although this loss appears to be substantial the decrease in thrust is only 11%.

FIGURE 3.6 EFFECT OF MIXING LOSS ON THRUST

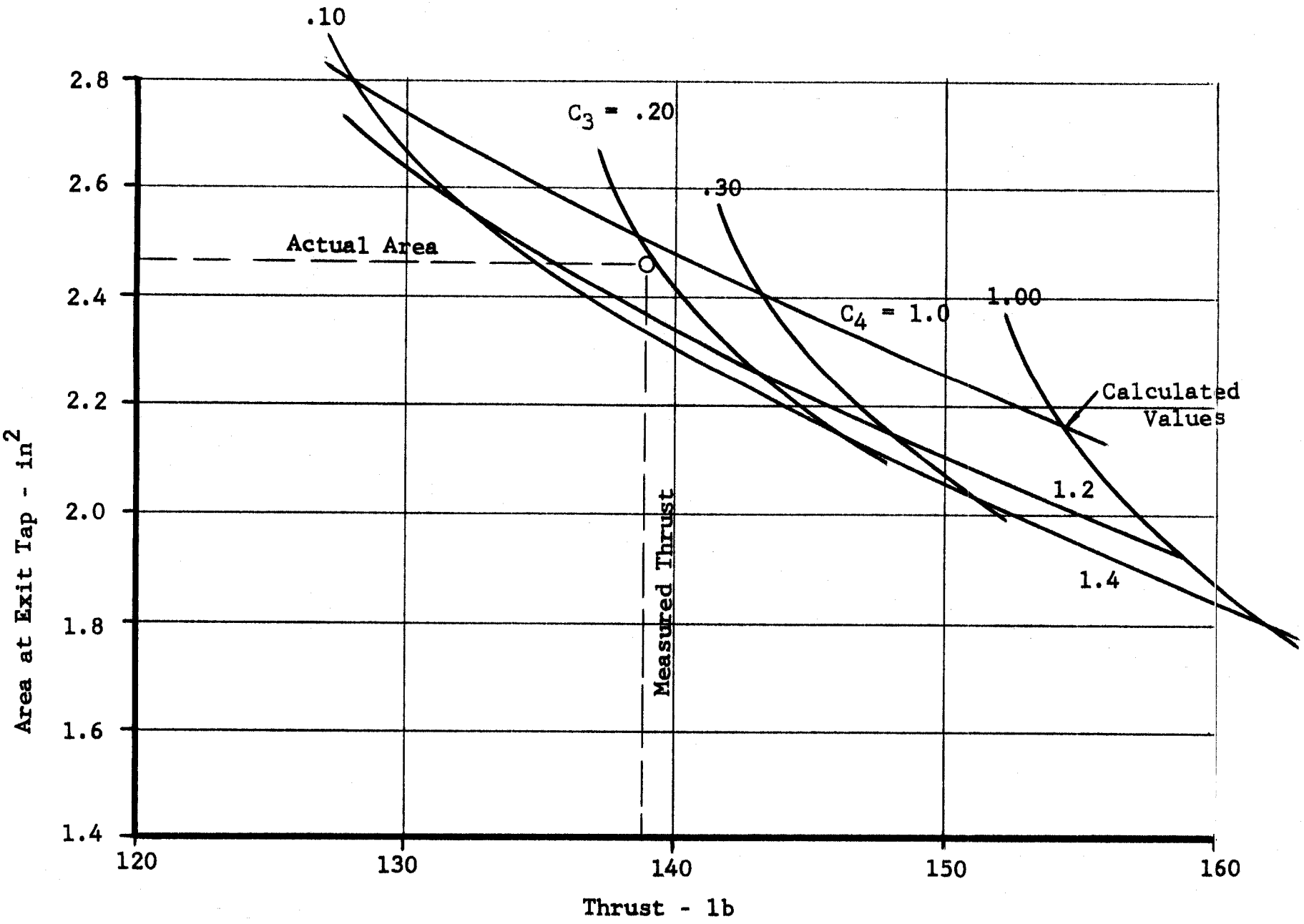

SECTION 4

TEST NO. 2 - SIX INJECTION PORTS WITH MODULATED INJECTED FLOW

4.1 Test Results

After the design modifications had been completed, it was decided to vary the mass flow and hence the chamber pressure of the secondary injectors during the firing. This and the following sections present the analysis of the data from the subscale firing of the 37.5:1 area ratio nozzle compensated by six secondary injectors varying in operation from 10 to 100 percent of the chamber pressure and mass flow of the main nozzle.

The measured axial thrust was increased 60 percent due to the secondary injection and the exit pressure was increased to nearly ambient pressure at 100 percent secondary injection. Further elaboration on the results of the test are contained in the following sections.

The dimensions of the 37.5:1 altitude nozzle, position of the injection nozzles and the location of the static pressure taps are shown in Figure 4.1.

4.1.1 Static Pressure Measurements - Hot Test

The nominal horizontal locations of the pressure taps from the throat were:

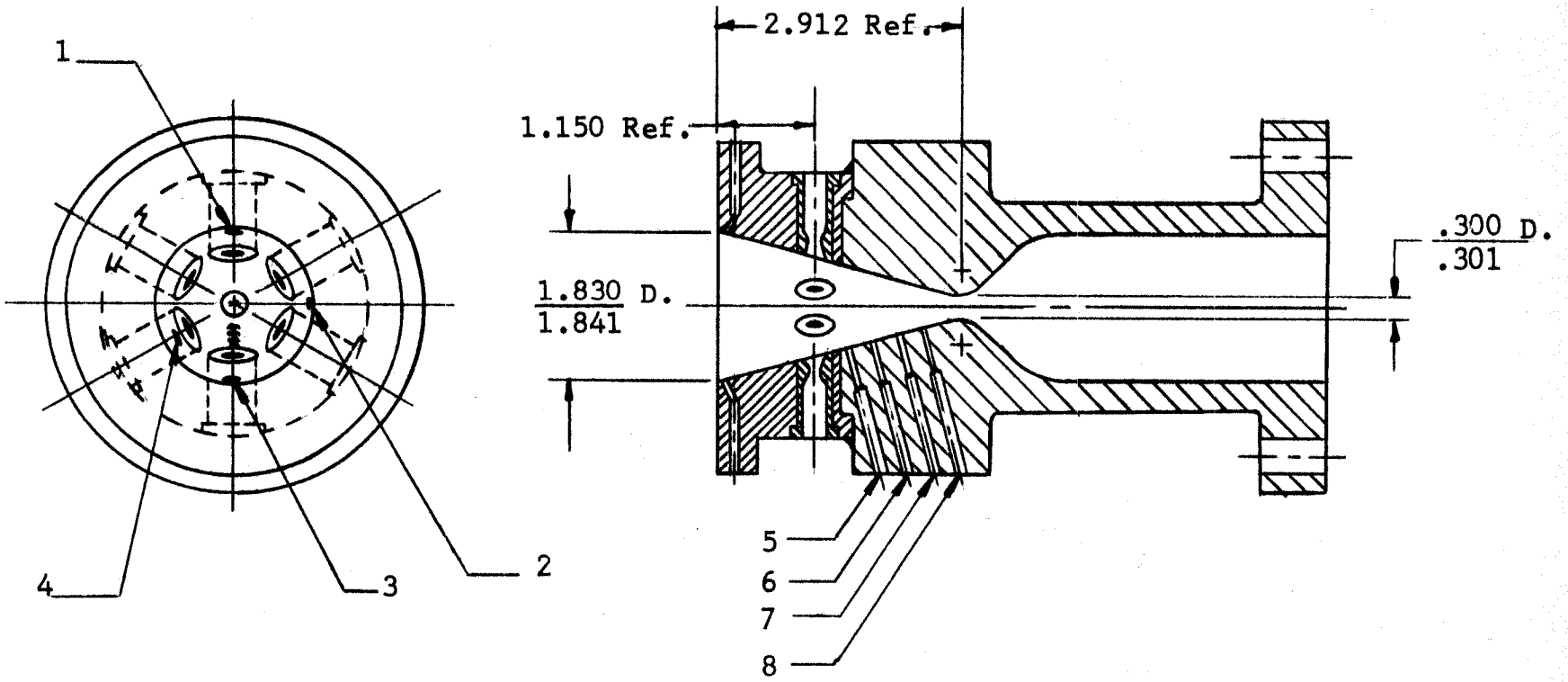

FIGURE 4.1

STATIC TAP LOCATIONS

#8 - 0.505 in.

#7 - 0.817 in.

#6 - 1.129 in.

#5 - 1.441 in.

#4 - 2.539 in.

#1 - #3 - 2.822 in.

Table 4.1, Figures 4.2 and 4.3, contain samples of these pressure measurements. They were checked for correlation with the recorded primary chamber pressure of 955 psia (10 sec.) prior to the ignition of the secondary injection system. Figure 4.4 is the plot of this data. It can be seen that the theoretical and actual pressure distribution agree very closely.

With the secondary generator ignited, the pressure within the primary nozzle upstream of the injectors increased from the range of 7-20 psia to approximately the range of 47-36 psia. The trend with time of the pressure indicated that tap #8 was unaffected and that tap #7 pressure was slowly raised to its value of 36 psia at 28.3 seconds. It is felt that this was due to the possibility of the formation of a lambda shock structure influencing the pressure reading upstream of the initial shock apex.

TABLE 4.1

PRESSURE TAP MEASUREMENTS

w/w$_o$	Time (Sec)	#1 (PSIA)	#2 (PSIA)	#3 (PSIA)	#4 (PSIA)	#5 (PSIA)	#6 (PSIA)	#7 (PSIA)	#8 (PSIA)
Primary Nozzle Only	0	14.81	14.81	14.81	14.81	14.81	14.81	14.81	14.81
	5	13.69	13.69	13.45	13.57	6.49	11.25	19.56	34.12
	10	13.69	13.57	13.51	13.32	6.94	11.54	19.56	35.01
100%	15	13.57	13.32	13.32	14.81	45.70	40.35	20.16	34.71
100%	20	12.83	13.69	13.51	15.80	48.08	40.65	23.72	35.01
100%	25	13.20	13.45	13.45	15.06	47.48	40.95	37.98	34.71
100%	28	13.69	13.57	13.45	14.56	46.89	40.65	36.79	34.86
100%	28.3	13.69	13.45	13.38	14.56	46.59	40.65	36.20	34.71
90%	28.68	13.57	13.32	13.32	14.31	43.32	38.57	30.26	34.71
80%	29.10	13.20	13.07	13.14	13.69	39.31	34.41	29.66	34.71
70%	29.53	13.01	12.64	12.95	13.07	33.82	29.36	26.10	35.01
60%	29.97	12.33	12.27	11.83	12.14	26.99	24.31	24.02	35.01
50%	30.38	11.28	12.08	10.91	11.59	21.34	19.56	22.53	35.01
40%	30.82	10.16	12.89	10.10	11.96	16.89	16.00	21.34	35.01
30%	31.25	10.60	12.70	10.60	11.46	14.22	14.07	20.75	35.01
20%	31.67	12.77	12.64	12.77	11.96	13.18	13.32	20.16	35.01
13%	32.00	14.00	12.83	13.63	13.01	13.32	13.03	20.01	35.01
10%	33.00	13.51	12.83	14.81	12.95	11.39	12.14	18.82	34.86

Barometric Pressure - 14.81 psia

More numbers to [illegible]

FIGURE 4.2 COMPARISON OF THEORETICAL AND MEASURED STATIC PRESSURE BEFORE AND AFTER SECONDARY INJECTION

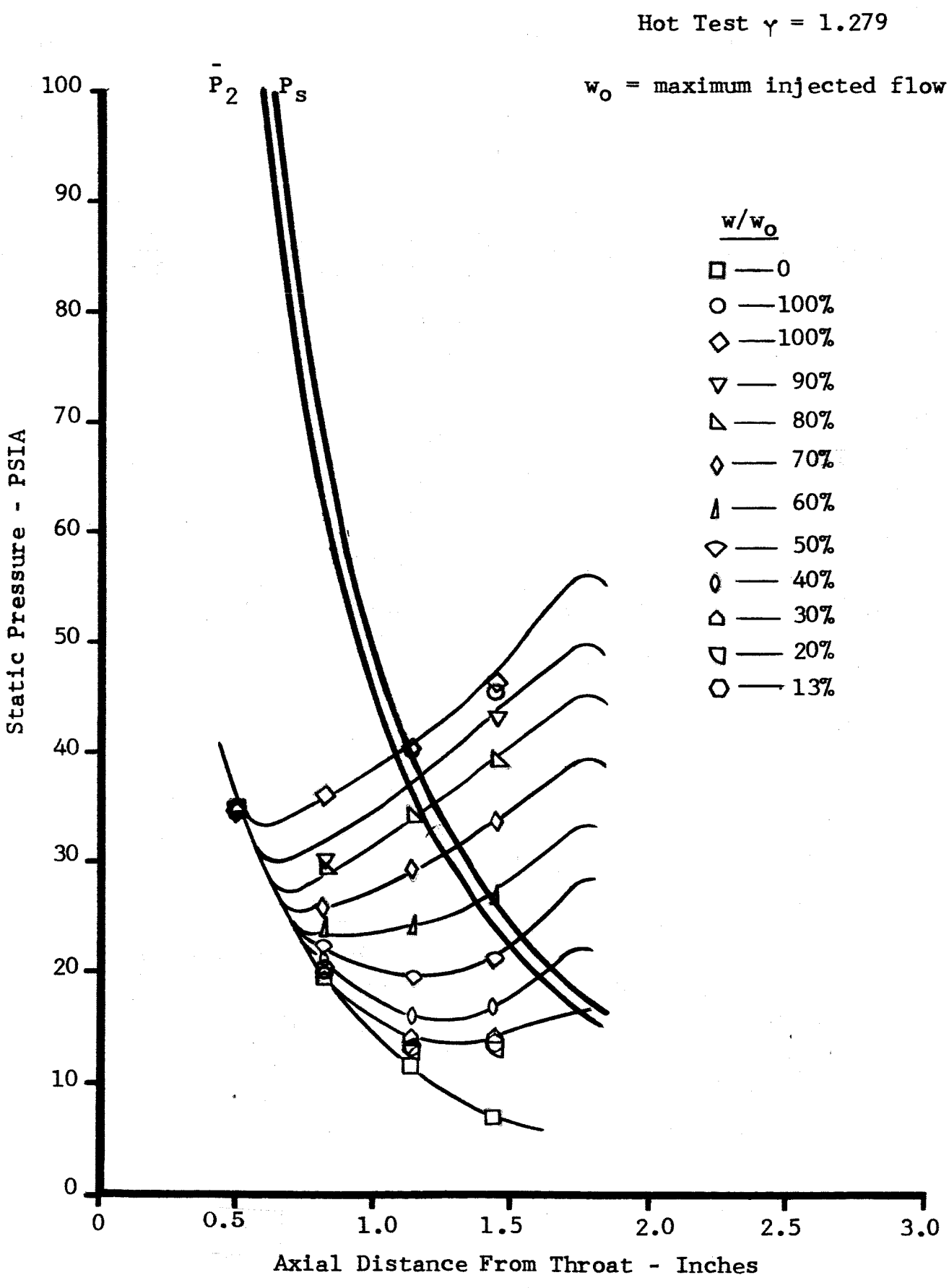

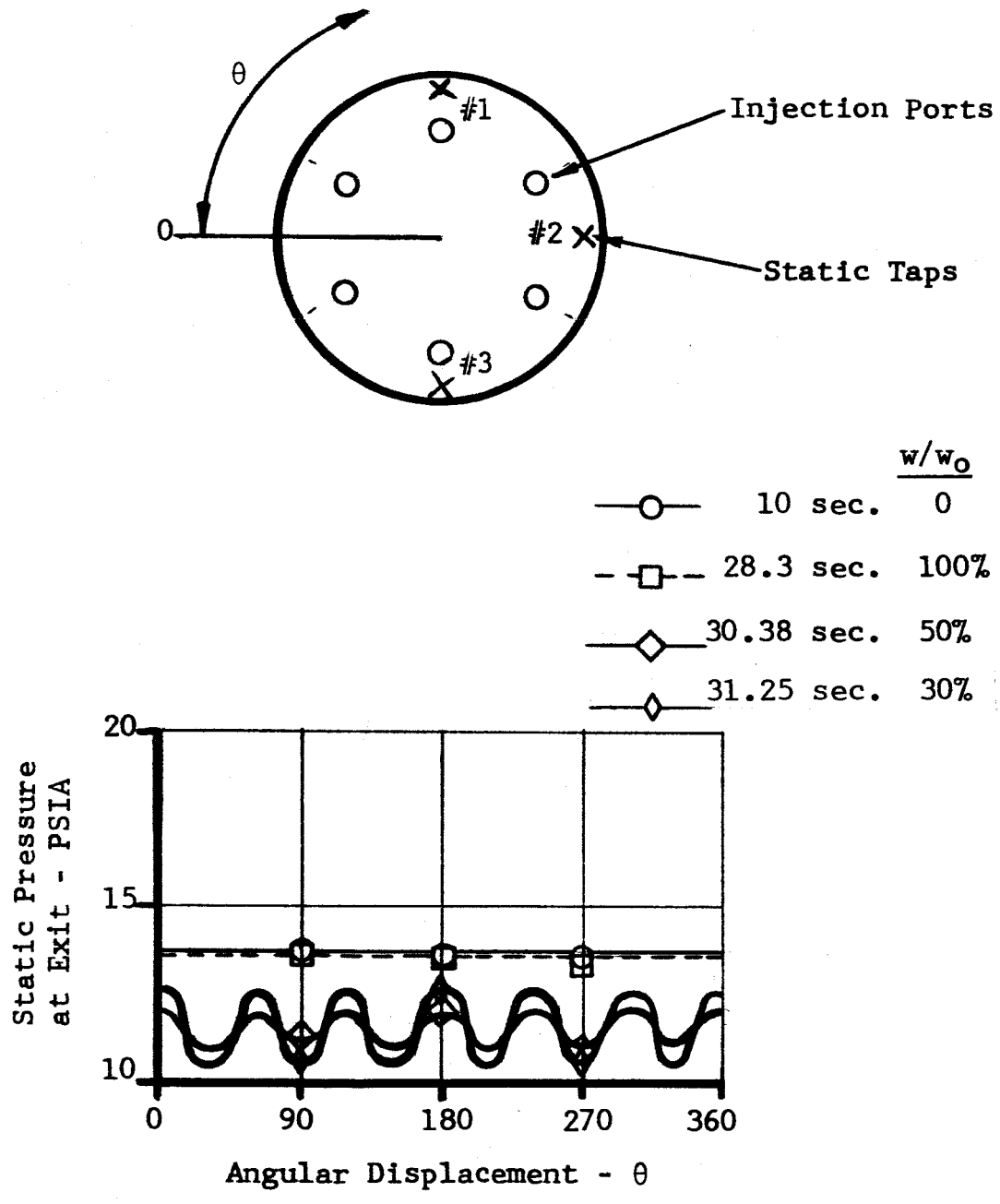

FIGURE 4.3

PERIPHERAL DISTRIBUTION OF STATIC PRESSURES AT EXIT OF PRIMARY NOZZLE

FIGURE 4.4 MACH NUMBER AND PRESSURE DISTRIBUTION BEFORE SECONDARY INJECTION

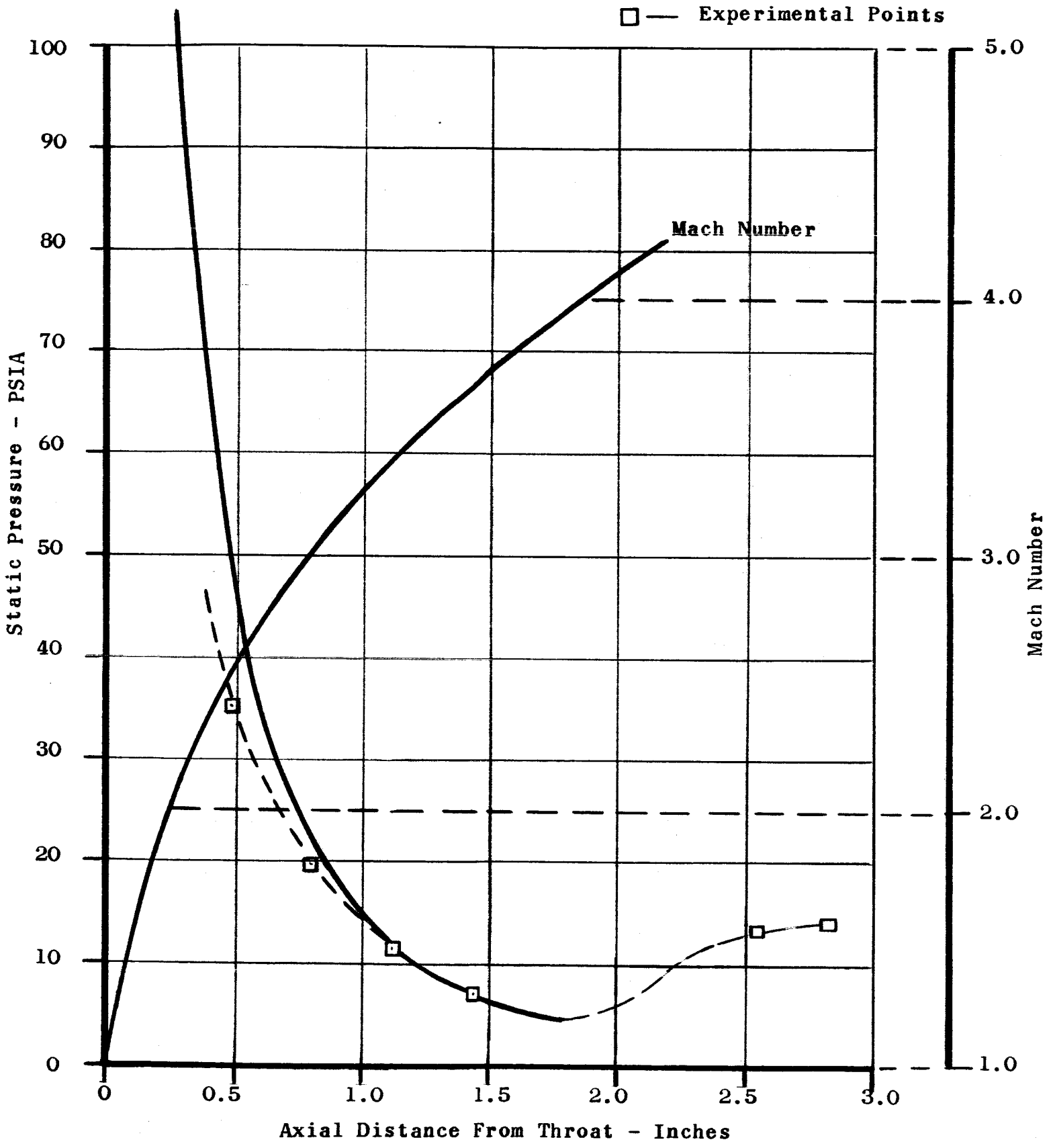

The theoretical injectant pressure was 57.0 psi at 100 percent secondary flow. As can be seen by the pressure plotted in Figure 4.2, this pressure was higher than the pressure recorded at the pressure taps. It is possible that the injectors were located too far upstream because the pressures recorded in cold tests prior to the hot firing do not exhibit this tendency. Additional comments will be made in later sections. Once this pressure distribution was established, reducing the injectant pressure and mass flow did not disturb this trend. Unfortunately, when the injectant pressure was increased two of the pressure taps (#5 and #7) were lost and did not record. Therefore, no trends could be noted on this swing from low to high injectant pressure. The pressure at the exit taps (#1 and #3) were compensated to nearly ambient pressures at 100 percent secondary injection. The lowest exit pressure recorded was 10 psia at 35 percent secondary injection. At lower injection rates a pressure rise was recorded at the exit indicating a beginning of separation of the secondary injection flow within the nozzle.

The circumferential pressure distribution was improved with the use of six injectors (Figure 4.3.) The exit plane taps recorded

approximately the same pressure down to 40 percent secondary injection at which point tap (#2) located between the injectors indicated a higher value than taps (#1 and #3) in line with injection ports. This increase can be attributed to loss of compensation between the injectors.

4.1.2 Thrust Measurements

In the measurement of thrust there was a one second time delay filter in the recording of the thrust trace. The output delay was approximated and corrections applied to the thrust measurements. The resulting thrust measurements corresponding to time are presented in Table 4.2 and Figure 4.5. The primary thrust level recorded was 82 pounds and the maximum combined thrust was 138 pounds.

4.1.3 Specific Impulse (I_{sp})

The augmented thrust measurements were used to calculate the specific impulse of both the combined primary and secondary system and the secondary system by itself.

For the combined system the I_{sp} was determined by dividing the total augmented thrust by the sum of the primary flow and the injected secondary flow. A plot of this I_{sp} for varying amounts

TABLE 4.2

THRUST LEVEL VARIATION

w/wo	Time (Sec)	P Primary PSIG	P Inj. PSIG	Thrust Lb.
Primary	0	0	0	0
Nozzle	5	890	0	77
Only	10	940	325	82
100%	15	980	860	131
100%	20	990	910	137
100%	25	995	940	138
100%	28	1000	940	138
100%	28.3	1000	920	138
90%	28.68	1000	820	128
80%	29.10	1000	735	123
70%	29.53	1000	640	112
60%	29.97	1005	540	103
50%	30.38	1005	460	98
40%	30.82	1010	360	93
30%	31.25	1010	265	91
20%	31.67	1015	180	90
13%	32.00	1015	110	90
10%	33.00	1015	85	90

FIGURE 4.5 THRUST MEASUREMENTS

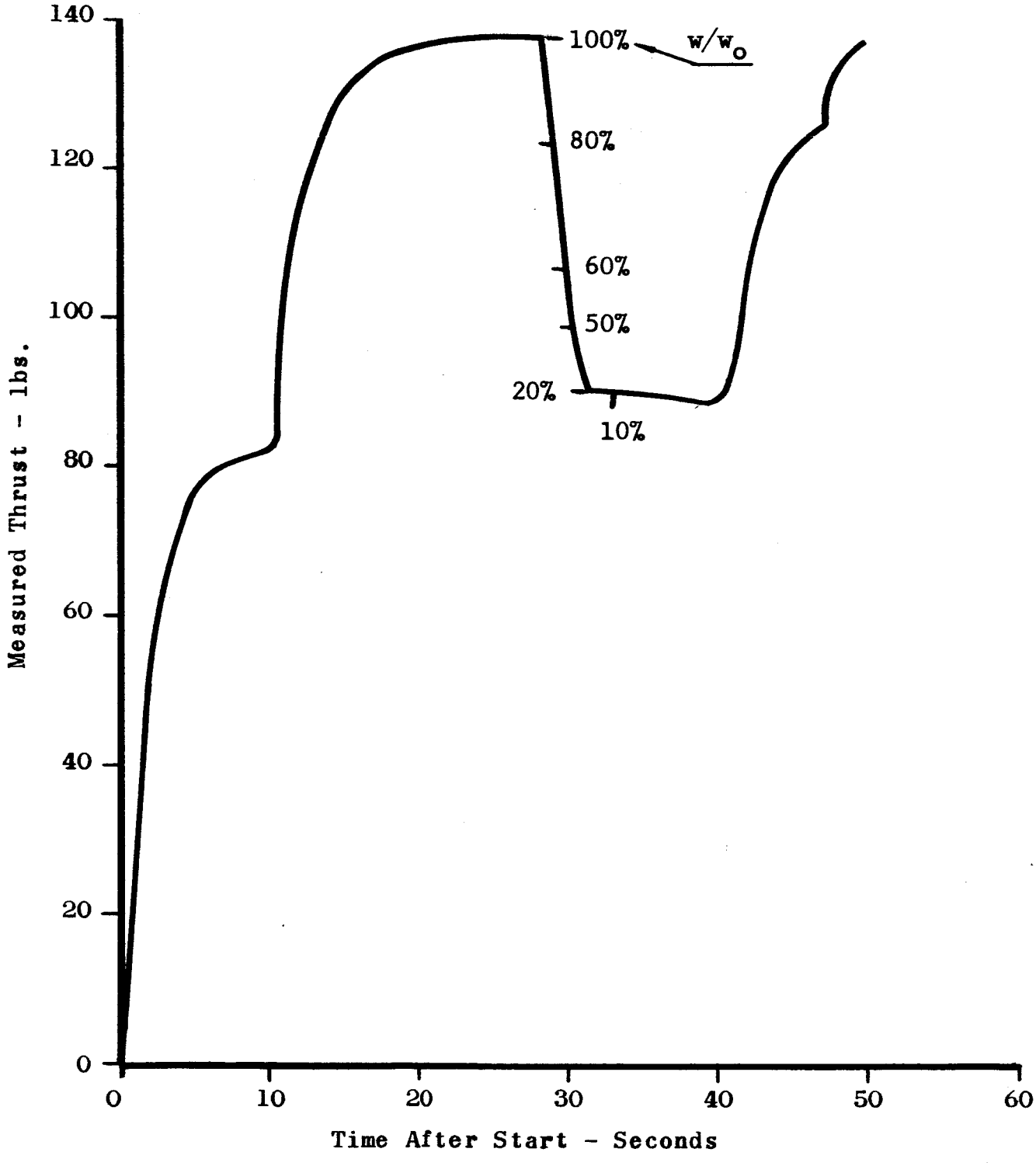

of injected flow is shown in Figure 4.6. The curve is reasonably flat for injected flow values between 40% and 100%. At injected flows below 40% the I_{sp} increases to its maximum of 150 secs. at zero injected flow.

The I_{sp} of the secondary system was calculated by dividing the thrust augmentation (i.e. the total augmented thrust minus the thrust due to the primary flow) by the amount of injected mass flow. This is plotted in Figure 4.7. There appears to be very little thrust hysteresis between increasing and decreasing secondary flow. The discrepancies occurring at low flow values are attributed to the relative magnitude of instrumentation errors with respect to absolute flow levels.

4.1.4 Secondary Mass Flow Variation

The secondary mass flow variation with time can be found from the secondary pressure and temperature measurements applied in the following equation for gas flow through a choked orifice.

$$w = A^* P_t C_d \sqrt{\frac{kg}{T_t R \left(\frac{k+1}{2}\right)^{\frac{k+1}{k-1}}}} = \frac{.420\ A^* P_t}{\sqrt{T_t}}$$

The resultant curve is shown in Figure 4.8.

FIGURE 4.6 COMBINED SYSTEM SPECIFIC IMPULSE VARIATION WITH SECONDARY MASS FLOW

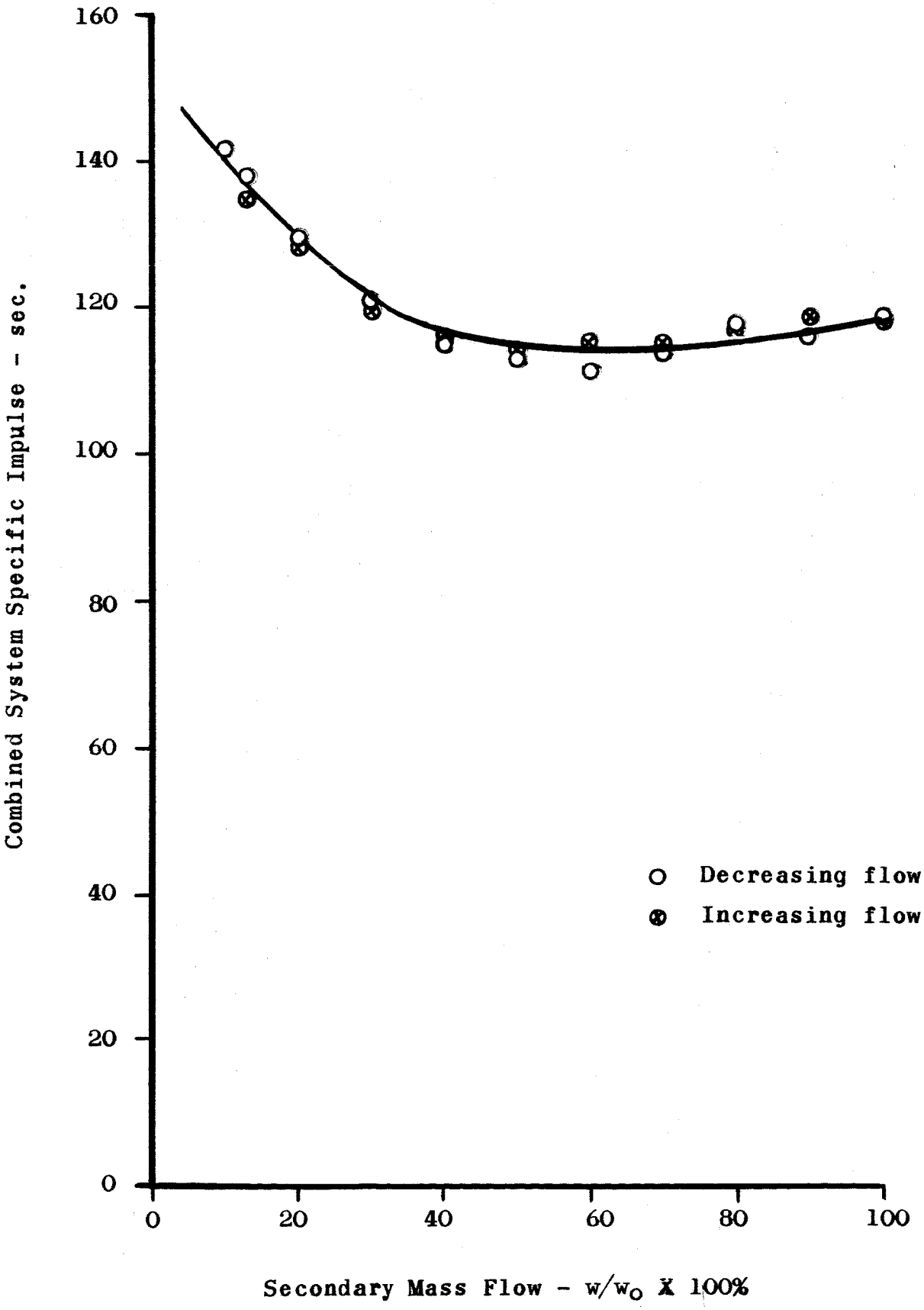

FIGURE 4.7 SECONDARY SYSTEM SPECIFIC IMPULSE VARIATION WITH SECONDARY MASS FLOW

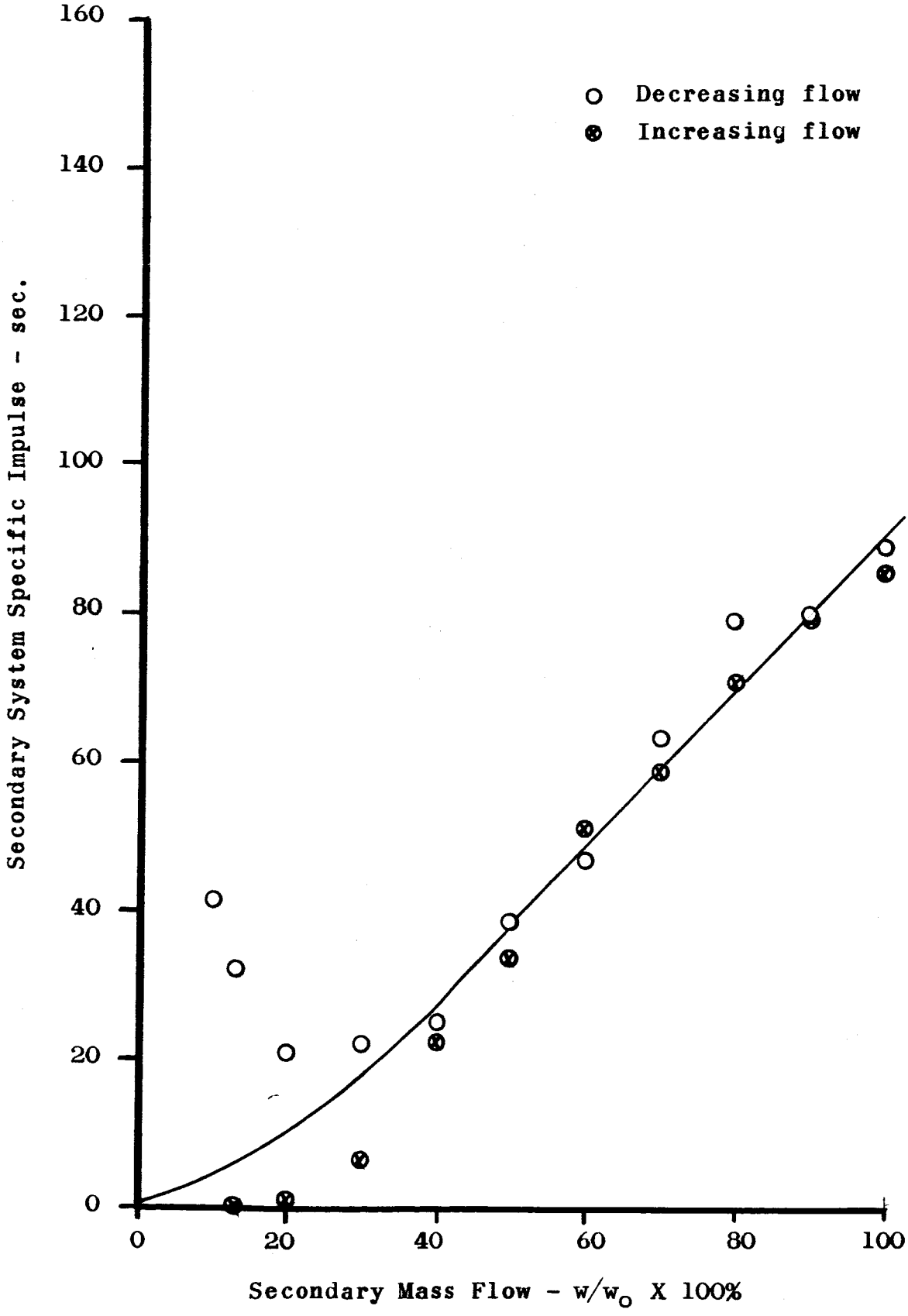

FIGURE 4.8

SECONDARY MASS FLOW VARIATION WITH TIME

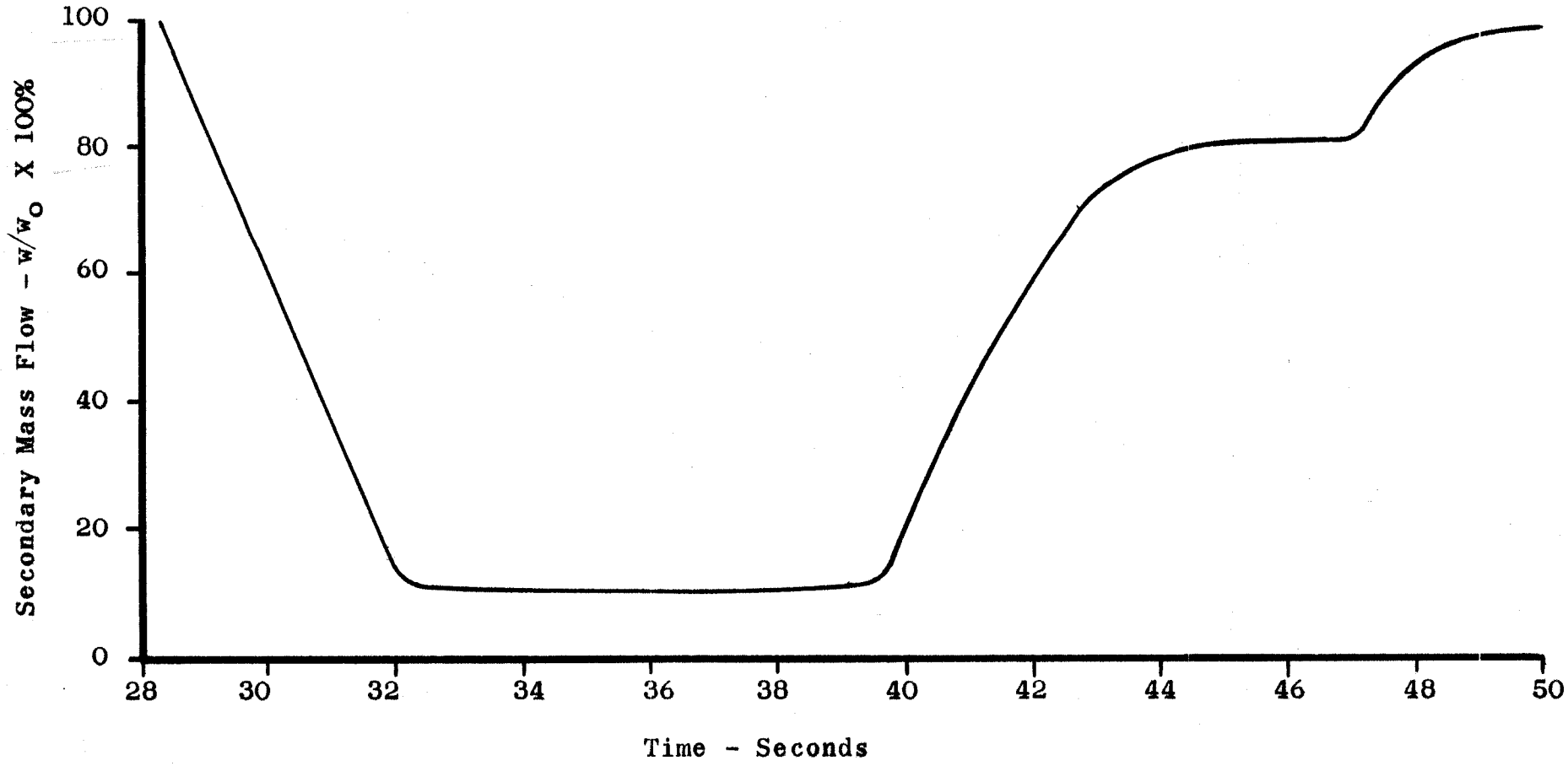

4.1.5 Static Pressure Measurements - Cold Test

The same nozzle configuration was used in the cold test. Pressures were recorded at these taps throughout the test. Figure 4.9 contains a sample of these pressures.

The nitrogen system is not capable of handling the flow of both the primary and secondary systems at 1000 psi. Therefore, the primary nozzle was run alone at 1000 psia. Its pressure data is presented in Figure 4.9 and checked favorably with the theoretical pressure distribution.

The combined mass flow necessitated a drop in the upstream pressure to approximately 700 psia. The theoretical pressure distribution is also plotted in Figure 4.9. Tap #8 is unaffected by the secondary injection and its pressure correlates with theory.

The theoretical injectant pressure was 37 psia at the 100 percent secondary flow. This pressure agrees favorably with the pressure measurements of the taps located upstream of the injectors and the separation pressure, P_s, based on the calculated Mach number. This value is also plotted on Figure 4.9.

FIGURE 4.9 COMPARISON OF THEORETICAL AND MEASURED STATIC PRESSURES BEFORE AND AFTER SECONDARY INJECTION

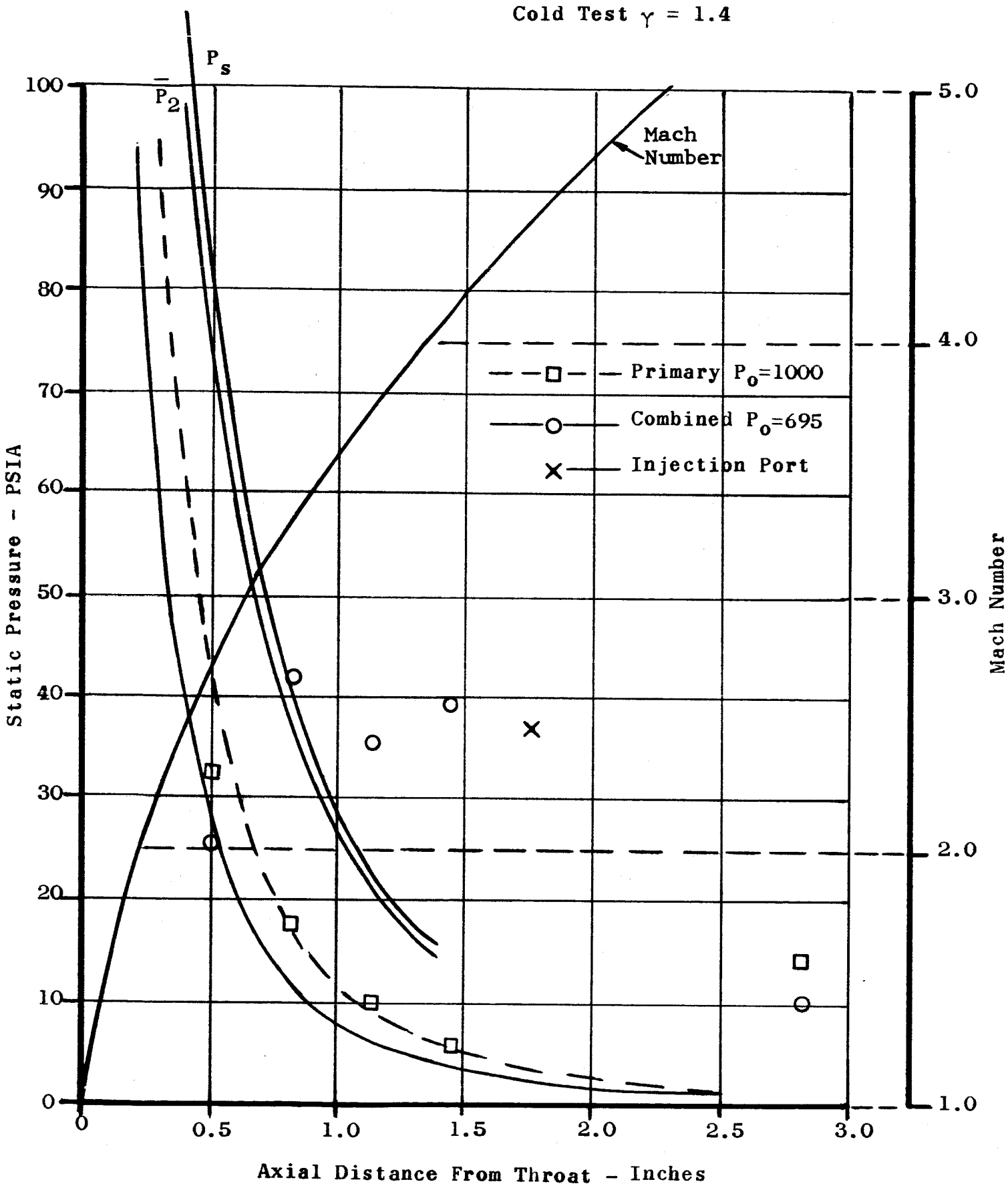

The pressure at the exit taps (#1 and #3) was compensated to approximately 10 psia. The circumferential distribution was also excellent. No analysis was made of other percentages of injected flow using N_2.

4.2 Correlation with Analytical Model for Supersonic Injection Into Supersonic Mainstream

The analytical model for the 37.5:1 area ratio subscale nozzle is presented in Appendices A and B.

Table 4.3 is a summary of values recorded throughout the valve cycling time.

As can be seen, these values are very close to the assumed values for the six injector design.

Table 4.3
System Properties 28-32 Seconds After Primary Ignition

	Primary Nozzle	Injection System
Weight Flow (lb/sec), w	.583	.058-.580
Nozzle Chamber Pressure (psia), P_c	1015-1030	100-955
Chamber Temperature (^oR), T_c	2370	1915-2080
Gas Constant, $\frac{ft.lb.}{lbm\,^oR}$, R	80.3	80.3
Ratio of Specific Heats, γ	1.279	1.279

4.2.1 Calculation of Exit Area and Thrust Based on Adjusted Value of P_{3_t} and P_{4_t}

The total pressure loss across the shock was approximated as 15 percent for the primary nozzle. Because the separation pressure and resultant shock location could not be readily determined for the test, the injector exit pressure was used as the P_{4_t} pressure value. Following the calculation procedure outlined in Appendices A and B, the results are shown in Table 4.4. A plot was also made showing the comparison between the hot test calculated and measured values of thrust and exit area, see Figure 4.10.

4.2.2 Estimated Mixing Losses Between Primary and Secondary Flows

An attempt was made to approximate what mixing losses would achieve perfect correlation of the values of the actual and theoretical areas and thrust. The assumed values for primary and secondary total pressure at the exit were multiplied by constants C_3 and C_4, respectively. For the 100 percent secondary injection agreement could not be obtained (see Figure 4.11). For the 50 percent secondary injection agreement could not be obtained between the theoretical and measured values for both thrust and area. Figure 4.12 is the result of this calculation.

TABLE 4.4

CALCULATED FLOW PERFORMANCES OF SIX INJECTOR DESIGN

w/w_o	100%	90%	80%	70%	60%	50%	40%	Cold Test w/w_o=100%
P_{t3}	900	890	890	890	890	890	880	610
P_3	13.51	13.40	13.14	12.87	12.14	12.08	12.89	10.68
M_3	3.28	3.275	3.288	3.298	3.335	3.338	3.291	3.298
A_3	.565	.570	.579	.587	.612	.614	.588	.419
P_{t4}	57.0	50.9	45.7	39.9	33.8	29.0	22.8	37.2
P_4	13.51	13.40	13.14	12.87	12.14	11.10	10.13	10.68
M_4	1.626	1.555	1.494	1.416	1.340	1.292	1.118	1.465
A_{4total}	1.432	1.375	1.310	1.249	1.202	1.139	0.998	1.499
$A_{e\ calc}$	1.997	1.945	1.889	1.836	1.814	1.753	1.566	1.918
$A_{e\ actual}$	2.459	2.459	2.459	2.459	2.459	2.459	2.459	2.459
$\Gamma 3$	102.3	102.1	102.3	102.2	102.1	102.1	102.1	65.6
$\Gamma 4$	62.4	54.1	46.1	38.1	29.7	22.3	13.0	41.0
$\Gamma_{Total\ calc}$	164.7	156.2	148.4	140.3	131.8	124.4	115.1	106.6
$\Gamma meas$	138.0	128.0	123.0	112.0	103.0	98.0	93.0	95.0

FIGURE 4.10

COMPARISON OF HOT TEST CALCULATED AND MEASURED VALUES OF THRUST AND EXIT AREA

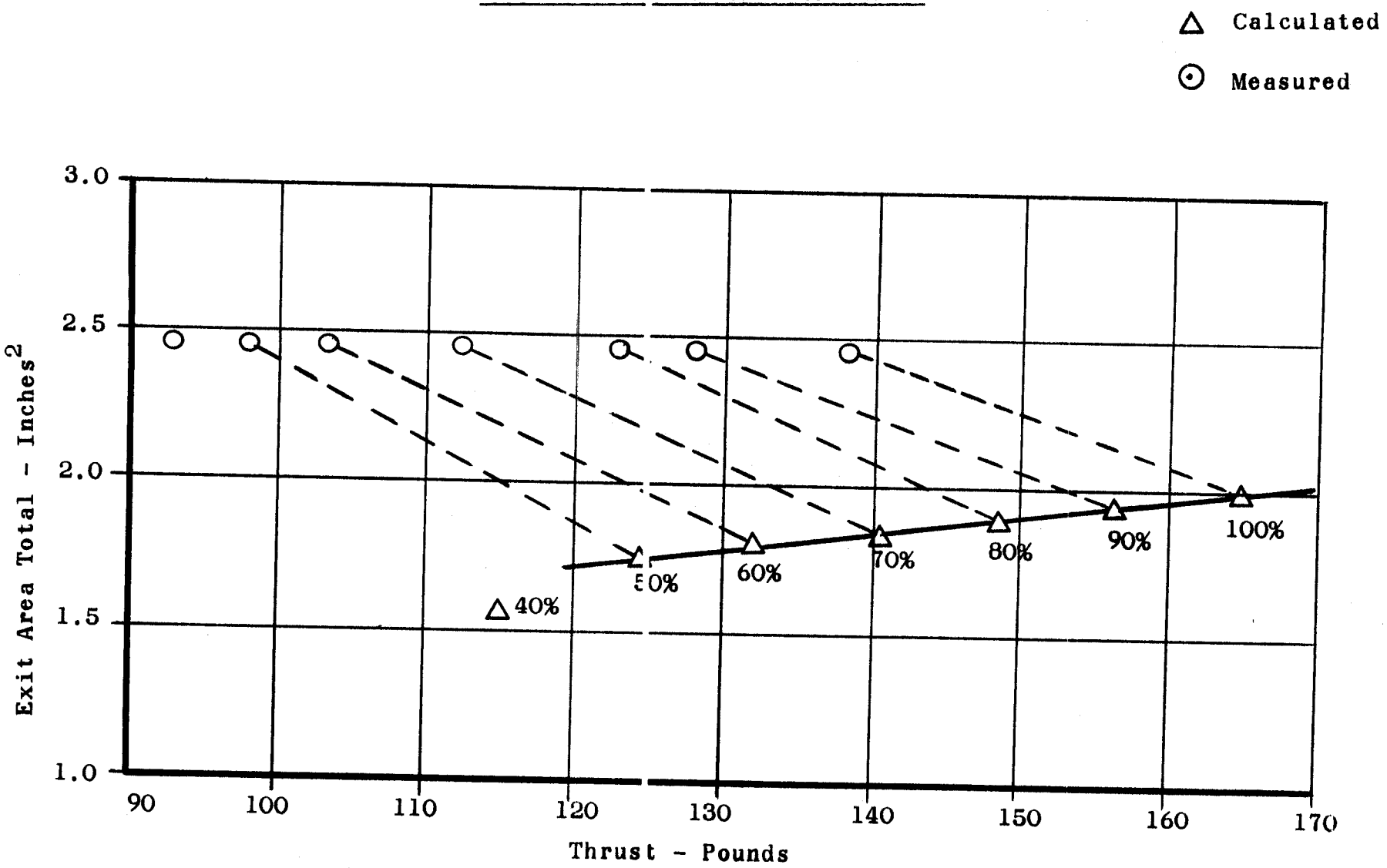

FIGURE 4.11

ESTIMATED LOSS - 100 PERCENT SECONDARY INJECTION

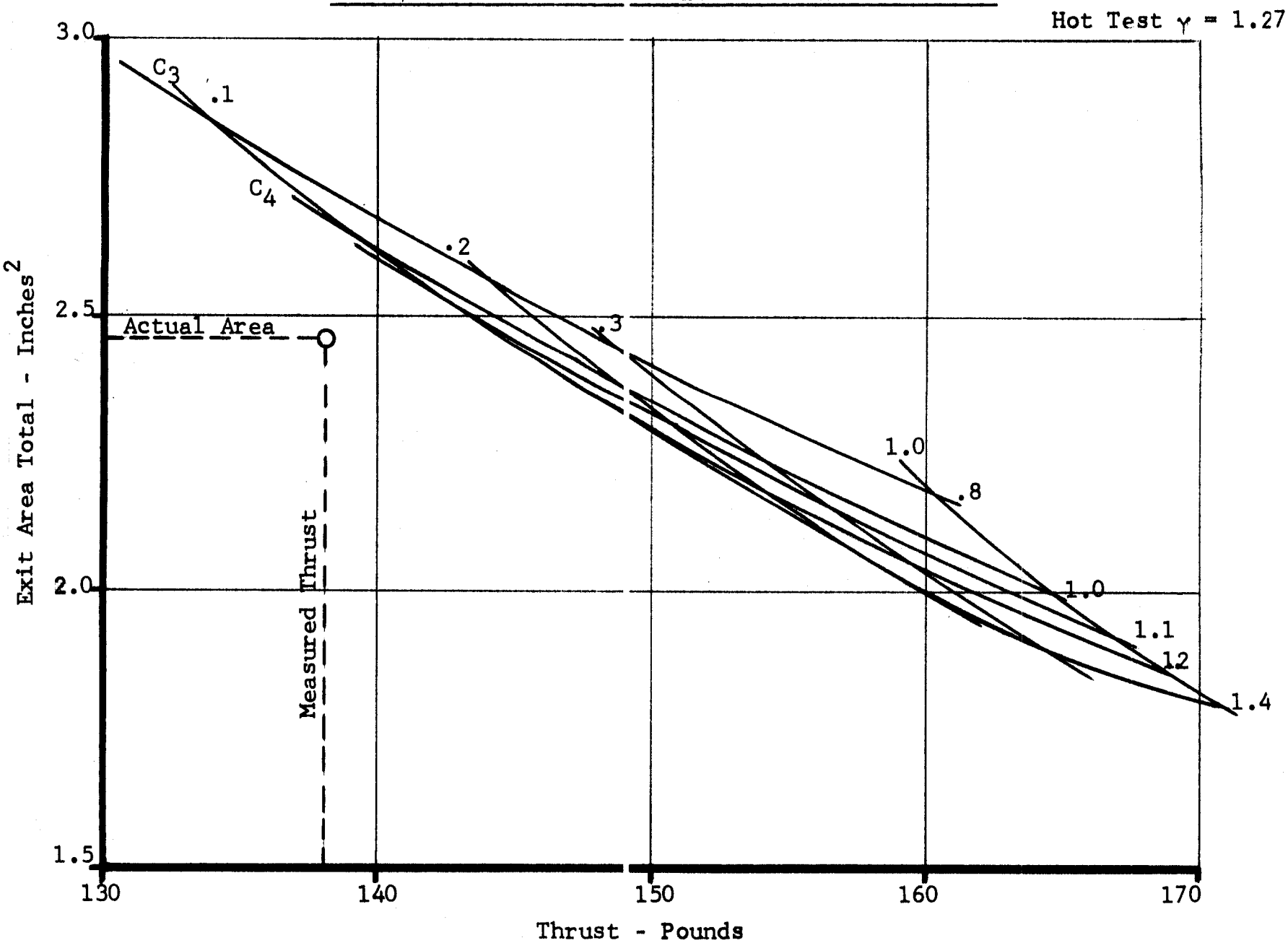

FIGURE 4.12 ESTIMATED LOSS 50 PERCENT SECONDARY INJECTION

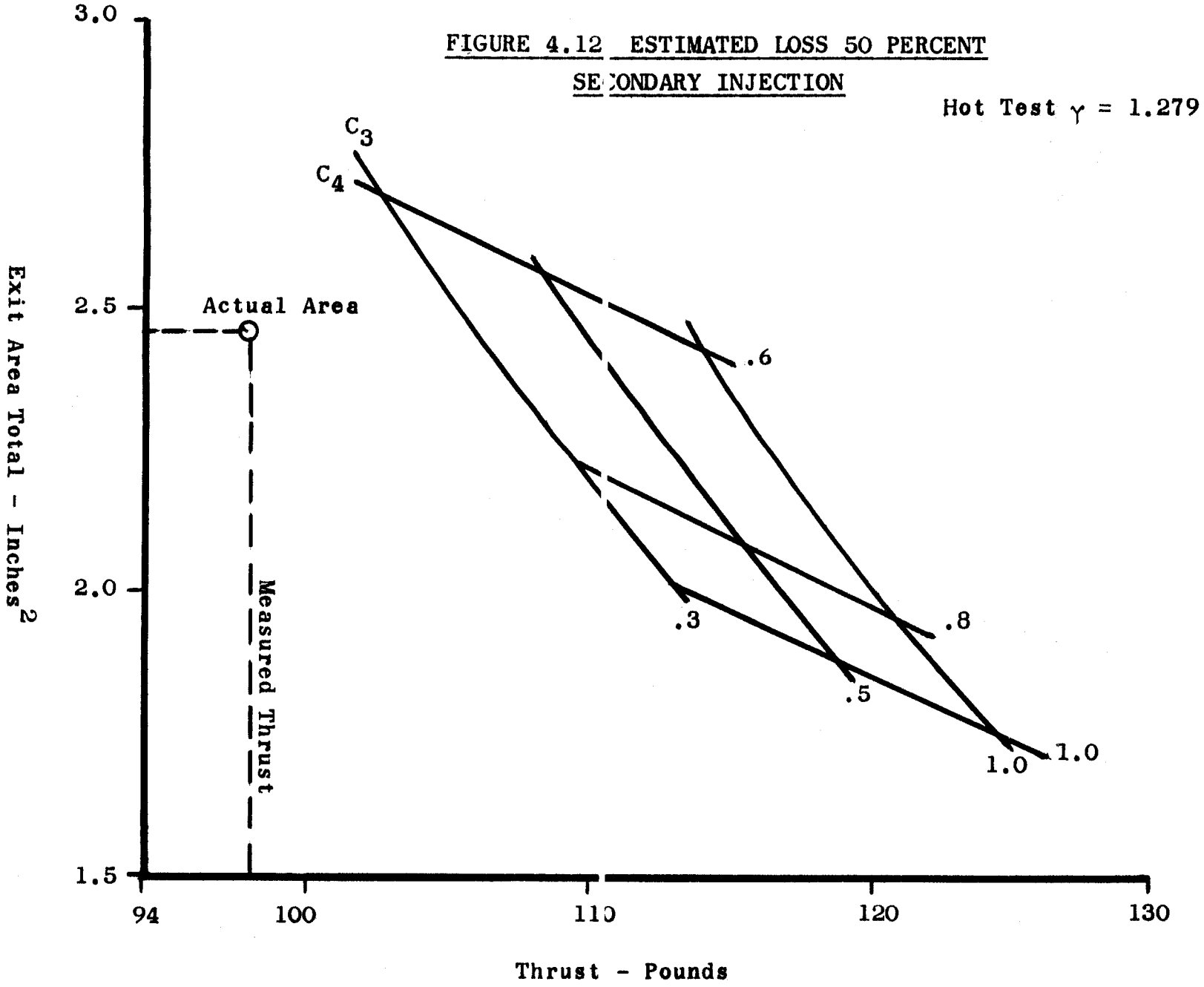

The cold test data was also analyzed for mixing losses (Figure 4.13.) A loss of approximately 30 percent on both the primary and secondary pressures resulted in a correlation of the theoretical and actual values of thrust and area.

4.2.3 Comparison of Hot and Cold Test Shock Apex

Dividing A_4 total by the number of injectors (6) determines the contribution of one injector to the area of the primary nozzle. The flow is assumed to take a hemi-cylindrical shape and the accomodation height, h, can be solved from geometry:

$$h = \left[\frac{2\ A_4\ \text{total}}{6\pi}\right]^{\frac{1}{2}}$$

The data obtained from the cold test indicated that the actual and theoretical separation pressures and injection pressure agree very favorably. Therefore, it was felt that the separation angle, δ, presented in Mager's paper was also accurate. The separation angle, δ, corresponding to $M_o = 3.37$ is 20.4^o. The calculated distance from the apex of the shock to the center of the injection port (perpendicular injection) depends on the separation angle and the accomodation height:

$$L_x = h\ (\cot \delta + \tan \alpha)$$

FIGURE 4.13 ESTIMATED LOSS 100 PERCENT SECONDARY INJECTION - COLD TEST

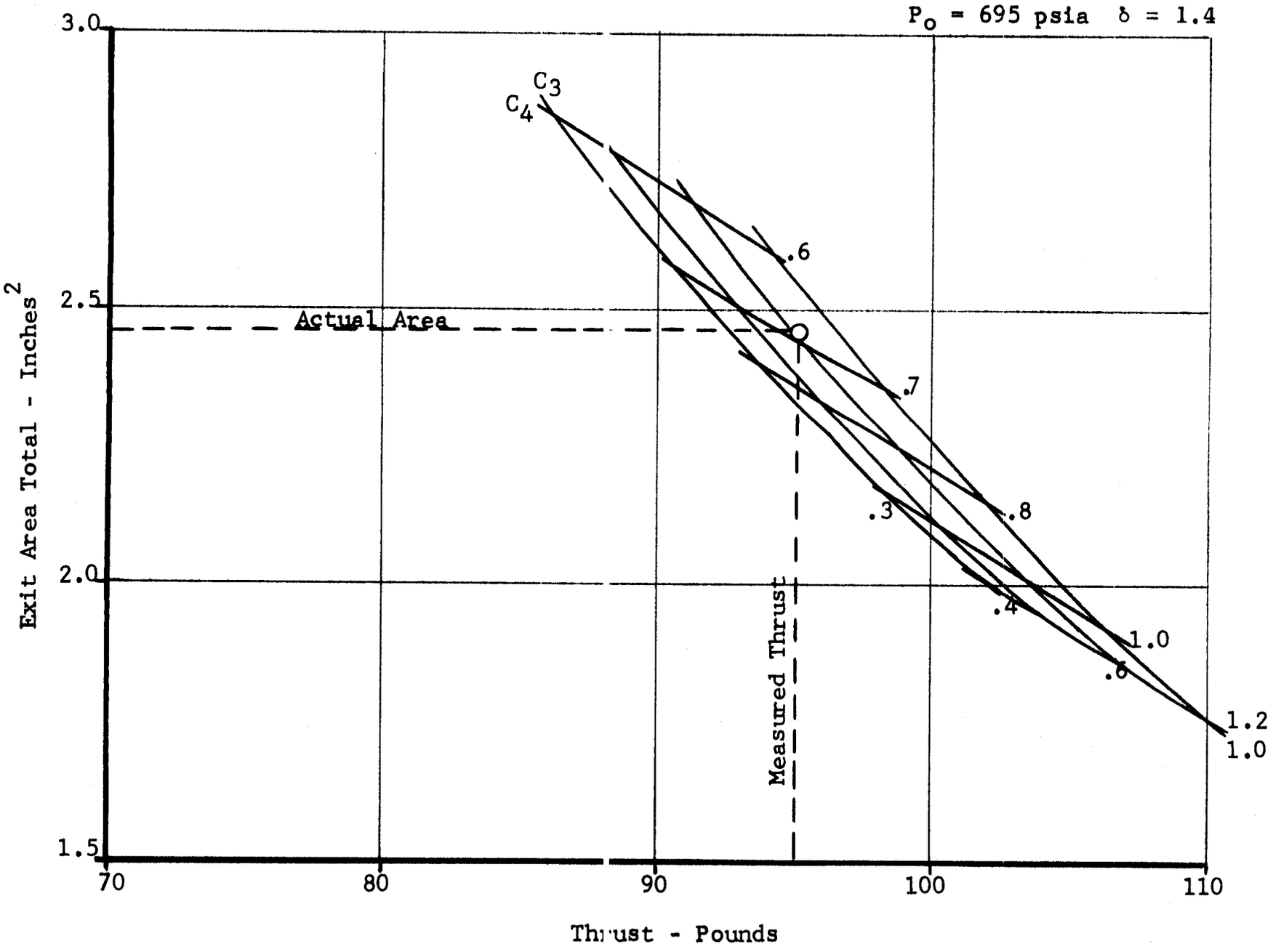

4.2.3.1 Cold Test

$$h = \left[\frac{2\ (1.499)}{6\pi}\right]^{\frac{1}{2}} = 0.399 \text{ in.}$$

$$L_x = .399\ [2.6889 + .26795]$$

$$= 1.180 \text{ in.}$$

and applying the modification suggested in Section 3.2.3.

$$L_x = .72\ h\ (\cot \delta + \tan \alpha)$$

$$= .849 \text{ in.}$$

This would agree very favorably with the assumed separation pressure position of 0.90 in. Of course, this is at a primary pressure of 700 psia in the primary and secondary pressures.

Assuming the primary and secondary pressures had been able to attain 1000 psia, the exit pressure of the secondary injector would have been 57 psia and the shock apex located at 1.12 in. from the throat.

4.2.3.2 Hot Test

The corresponding calculation for the hot test for 100 percent

assuming the separation would have occurred at 57 psia is:

$$h = \left[\frac{2\ (1.432)}{6\pi}\right]^{\frac{1}{2}} = 0.39 \text{ in.}$$

$$L_x = .39\ [2.6605 + .26795]$$

$$= 1.140 \text{ in.}$$

or applying the modification:

$$L_x = .72\ h\ (\cot \delta + \tan \alpha)$$

$$= 0.821 \text{ in.}$$

Since this calculation recognizes no other contribution than $A_{4\ \text{total}}$ and cot δ and the cot δ does not vary a great deal for its range of possibilities, the possibility exists that the injection port was placed too far upstream. This conclusion is based on the fact that the cold test demonstrated agreement with the shock apex location.

Another interesting facet is that for the first test and the present configuration cold test the injection port was located downstream of the natural separation point (4 psia minimum as recorded in the previous test). However, for the second hot

test the injection port was located upstream of this separation point and this could be contributing to some of the discrepancy in the pressures upstream of the injectors. This is demonstrated in Figure 4.14. The separation pressure (P_s) for the aforementioned tests was very nearly 14.7 psia.

FIGURE 4.14 NATURAL SEPARATION POINT COMPARISON WITH INJECTOR LOCATION

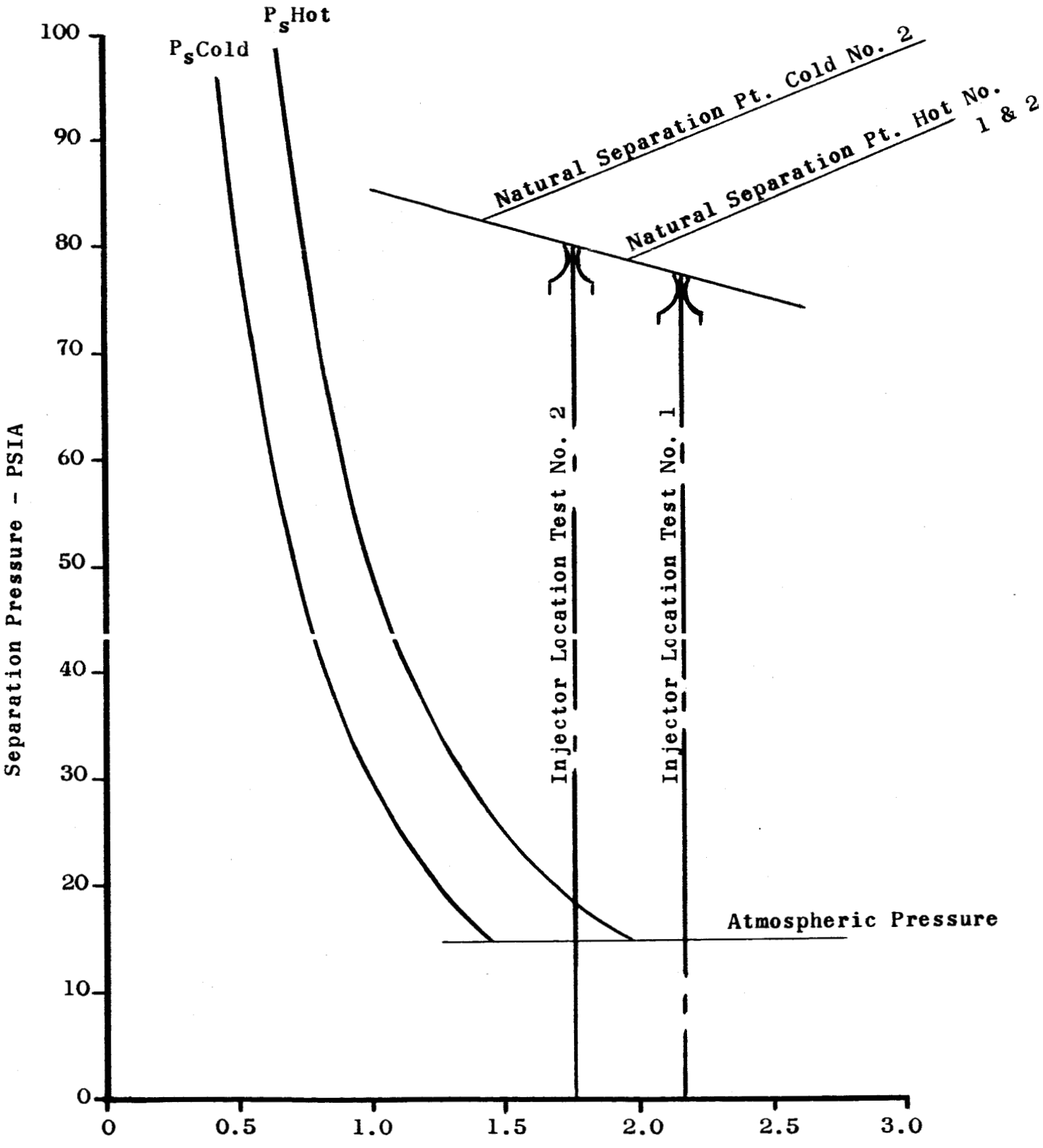

SECTION 5

CONCLUSIONS AND RECOMMENDATIONS

The experimental phase of this program has shown that a thrust augmentation of at least 60% of the axial thrust can be achieved by the injection of a mass flow, equal to the primary flow, into the nozzle expansion cone. This level of augmentation can be increased by optimizing the location and number of the injection ports. In addition a further increase could be obtained by injecting the gas in a downstream direction instead of perpendicular to the nozzle longitudinal axis.

From an efficiency point of view it seems that the optimum injected to primary flow ratio is about 40%. This flow ratio would also ensure consistent pressure compensation around the periphery of the nozzle exit plane.

The actual flow ratio required for a particular application would have to be determined by a study of the overall system since the level of thrust augmentation at 40% flow ratio may not satisfy the system requirements.

The analysis of the static pressure readings recorded during the second hot test shows that the injectors were not ideally located. For the first hot test and the cold test of the 6 injector configuration the injection ports were located downstream of the natural separation plane as determined by the nozzle pressure readings. However, for the second hot test the injection ports could have been upstream of this separation plane which could be contributing to some of the discrepancy in the pressures upstream of the injectors. A literature survey of the work carried out in this area indicated that a considerable amount of Schlieren analysis has been done on the injection of a gas into a supersonic stream, although none covered the conditions that existed during either of these tests.

Although it was possible to account for the difference between theoretical and experimental values for test No. 1 by assuming a certain percentage of mixing losses in the nozzle, this assumption was not validated by the second test.

The following recommendations are made for further study in this area.

1. Additional test firings to optimize the injector location and evaluate the performance of downstream injection.

2. Develop a more elaborate theoretical model using a semi empirical approach based on more detailed knowledge of the mixing between the two streams and the total pressures at the nozzle exit plane.

3. Evaluate the stability of the axial flow with secondary injection. This could be accomplished by visual observation methods of the exhaust gases.

4. Carry out a system study of a one stage to orbit vehicle, based on the parameters developed in this program and those recommended above. This would determine feasibility of this concept as opposed to multistage configurations.

APPENDIX A

ANALYTICAL MODEL

TEST NO. 1 - FOUR INJECTION PORTS WITH CONSTANT INJECTED FLOW

Description of the Mathematical Model

Because there is no complete understanding of the basic mechanisms of shock-boundary layer interactions, particularly when the boundary layer is turbulent, the construction of an analytical model for supersonic injection into a supersonic mainstream presents a very difficult problem. The model shown in Figure 1.a provides at least a qualitative description of the interactions involved.

Figure 1.a represents a section of the wall of a supersonic (expanding) nozzle in the neighborhood of an injection port. Far upstream from the point of injection, the mainstream expands with decreasing pressure as it flows along the outer edge of the boundary layer. There is no separation of the boundary layer and the mainstream is generally shock free.

At or near the point of injection, however, the boundary layer is deflected upward through an angle δ, producing a local change in mainstream direction with an accompanying shock pattern that creates a local adverse pressure gradient.

With injection the concept of boundary layer separation becomes

ambiguous since most of the criteria for separation are satisfied locally with even a small injection flow (for example, the limiting streamline of the main flow is detached from the channel wall). In order to relate the model to more conventional examples of separated flows, the injectant is assumed to enter in sufficient quantity to produce separation as conventionally as by a change in wall direction.

Under these conditions the boundary layer deflection (separation) angle, δ, is related to the upstream Mach number, M_o, by relations derived by Mager in Reference 4. With values of M_o and δ the shock angle and pressure ratio across the shock are determined by inviscid flow relations over a cone (the locally separated boundary layer is assumed to have a conical shape). To complete the model picture, the injected flow is assumed to enter with the same static pressure, P_j, as the pressure in the separated region, $\overline{P_s}$, and to be immediately turned to flow parallel to the nozzle wall without mixing. The location of the shock apex is determined from the assumed geometry.

Solutions Based on Estimation of Total Pressure in the Streams at the Nozzle Exit

It is the author's opinion that the integration of pressure forces to obtain momentum balances for the mainstream and secondary flows will not produce significant results with the information presently available. Furthermore, it would be very difficult to obtain measurements from which empirical adjustments

could be made to the analysis.

On the other hand, there is some basis upon which the total pressure in the flows at the nozzle exit can be estimated. Also measurements could be obtained much more readily (i.e. total pressure surveys at the nozzle exit) with which these estimates could be evaluated and corrected.

Total Pressure of the Mainstream at the Exit

If mixing between the two streams is neglected (as was done in the analyses of References 1 and 2) then the losses in the accelerating flow downstream from the induced shock should be quite negligible. Thus, the total pressure of the mainstream at the nozzle discharge should reflect only the losses occurring across the conical shocks induced by the secondary injection. This loss can readily be estimated from conical shock tables and the value of M_0 at the shock apex.

Estimated Total Pressure in the Secondary Flow at the Exit

After the secondary flow has entered the nozzle it is assumed to be turned to flow parallel to the nozzle walls. In actual practice this flow also should be accelerating and it is therefore assumed that most of the loss occurs in the turning and will amount to the dynamic head corresponding to the velocity component normal to the nozzle wall. Thus, in the present case little or none of the dynamic head of the secondary injectant will be recovered and,

$$P_{4_t} \approx P_j = P_s$$

i.e., the downstream total pressure should be approximately equal to the static pressure in the secondary jets.

Use of Exit Total Pressure to Calculate the Nozzle Flow Conditions

The flow in a nozzle with secondary injection can be determined, if in addition to the given mass flows and upstream stagnation state of the primary and secondary flows, four additional conditions are satisfied by the solutions. Two of these conditions are that continuity of mass flow must be maintained in each of the gas streams. In the past, investigators have chosen to utilize force-momentum balances for each stream to supply the additional two conditions required. For this study, however, the downstream total pressure has been used instead and enters into the calculations in the following way.

In the present case, it is intended to supply compensation to an altitude nozzle which will be sufficient to limit the exhaust static pressure, P_e, on the discharge plane to some prescribed value. In other words,

$$P_3 = P_4 = P_e \text{ (given)}$$

With P_{t_3} estimated and P_3 given, the Mach number of the mainstream at exit is readily determined from,

$$M_3 = \left\{ \frac{2}{\gamma-1} \left[\left(\frac{P_{t_3}}{P_e} \right)^{\frac{\gamma-1}{\gamma}} - 1 \right] \right\}^{1/2}$$

which can be inserted into the continuity equation to determine A_3.

Likewise, the Mach number of the secondary flow is given by,

$$M_4 = \left\{ \frac{2}{\gamma-1} \left[\left(\frac{P_{t_4}}{P_e} \right)^{\frac{\gamma-1}{\gamma}} - 1 \right] \right\}^{1/2}$$

which with continuity determines A_4. The application of these equations is demonstrated in the next paragraph.

It should be noted that neither the model suggested or the other available models have taken into account the effect of the injectant momentum on boundary layer deflection. Thus, they do not reflect the influence of the chamber pressure of the injector nozzles which should contribute significantly to the performance of the compensated nozzle.

Design Procedure

Table 1.a presents the initial design parameters for the primary nozzle and secondary injection system.

Four Injector Design

The variables involved in the calculation are presented in Figure 1.a.

	Primary Nozzle	Injection System
Weight Flow (lb/sec), w	0.615	0.615
Nozzle Chamber Pressure (psia), P_c	1000	1000
Chamber Temperature (°F), T_c	1810	1810
Gas Constant $\frac{\text{ft lb}}{\text{lb m °R}}$, R	84	84
Ratio of Specific Heats, γ	1.3	1.3
Nozzle Half Cone Angle (degrees), α	15	15
Throat Area (in^2), A*	0.070925	Design Consideration

TABLE 1.a SYSTEM PARAMETERS

The geometrical relationship between L_x and h for injection perpendicular to the centerline of the primary nozzle is given by:

$$L_x = h \left[\cot \delta + \tan \alpha\right]$$

The basic computing steps are given as follows:

1) assume a value of M_o
2) calculate A_o and P_o from the following equations:

$$A_o = \frac{A^*}{M_o} \left[\frac{1 + \tfrac{1}{2}(\gamma-1) M_o^2}{1 + \tfrac{1}{2}(\gamma-1)}\right]^{\frac{\gamma+1}{2(\gamma-1)}}$$

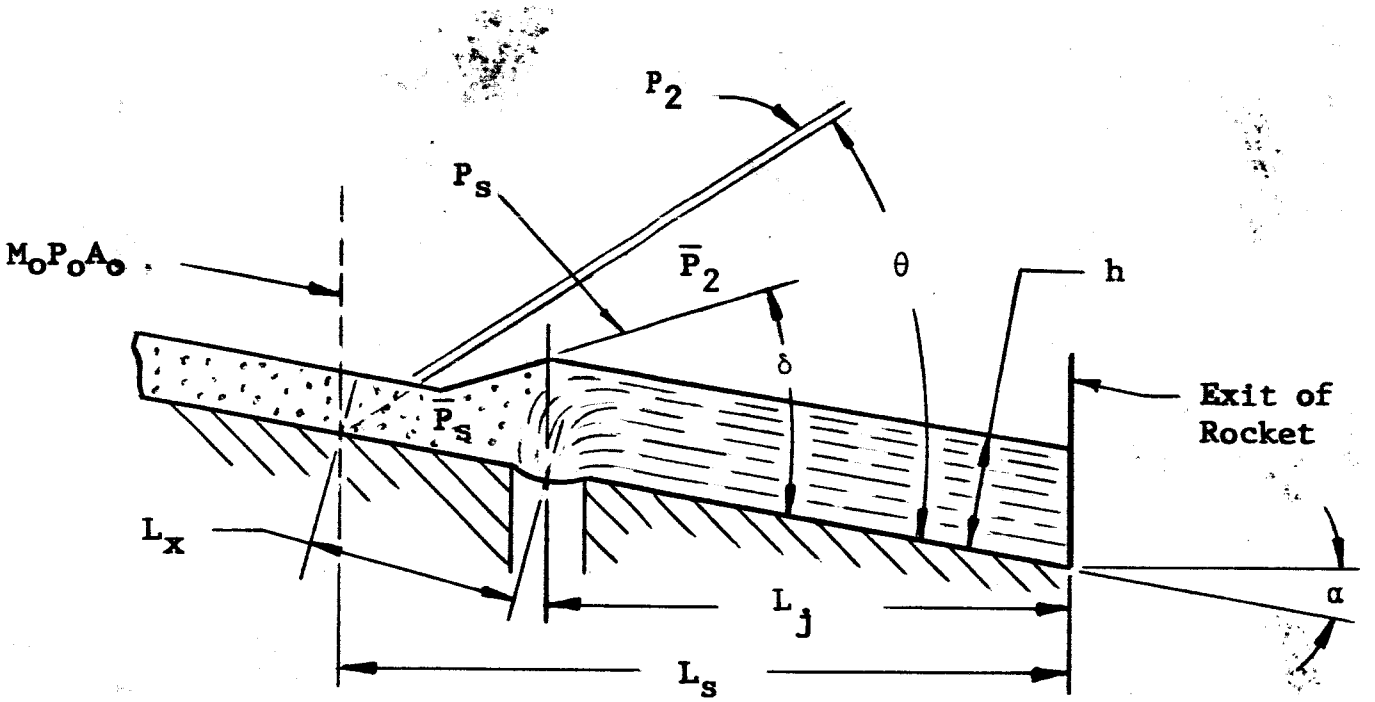

FIGURE 1.a SYSTEM VARIABLES

$$P_o = P_c \left[1 + \tfrac{1}{2} (\gamma-1) M_o^2 \right]^{\frac{\gamma}{\gamma-1}}$$

3) determine δ, θ, $\frac{\overline{P}_2}{P_o}$ and $\frac{P_s}{P_o}$ from Figure 2.a, Figure 2.a is the average of Figures 16 and 17 of Reference 2, which were determined for specific heat ratios of 1.2 and 1.4, respectively.

Based on Reference 5, the total pressure loss across the shock can be approximated as 5% for the range of conical separation angle found in Step 3. Therefore, the total pressure of the primary stream after the shock was assumed to be 950 psia rather than 1000 psia. The assumed loss in the secondary flow results in the separation pressure P_s, equal to P_{t_4}, the total pressure of the secondary flow. Experience has shown that a pressure of at least 50% of ambient pressure must be maintained at the nozzle exit to prevent separation inside the nozzle. Therefore, the desired exit pressure was taken as 8.0 psia for both the primary and secondary flows.

4) Calculate M_3, the Mach number at the exit of the primary flow from:

$$M_3 = \left\{ \frac{2}{\gamma-1} \left[\left(\frac{P_{t_3}}{P_3} \right)^{\frac{\gamma-1}{\gamma}} - 1 \right] \right\}^{\frac{1}{2}} \qquad \begin{aligned} P_{t_3} &= 950 \text{ psia} \\ P_3 &= 8 \text{ psia} \end{aligned}$$

5) Calculate A_3 from the continuity condition which gives,

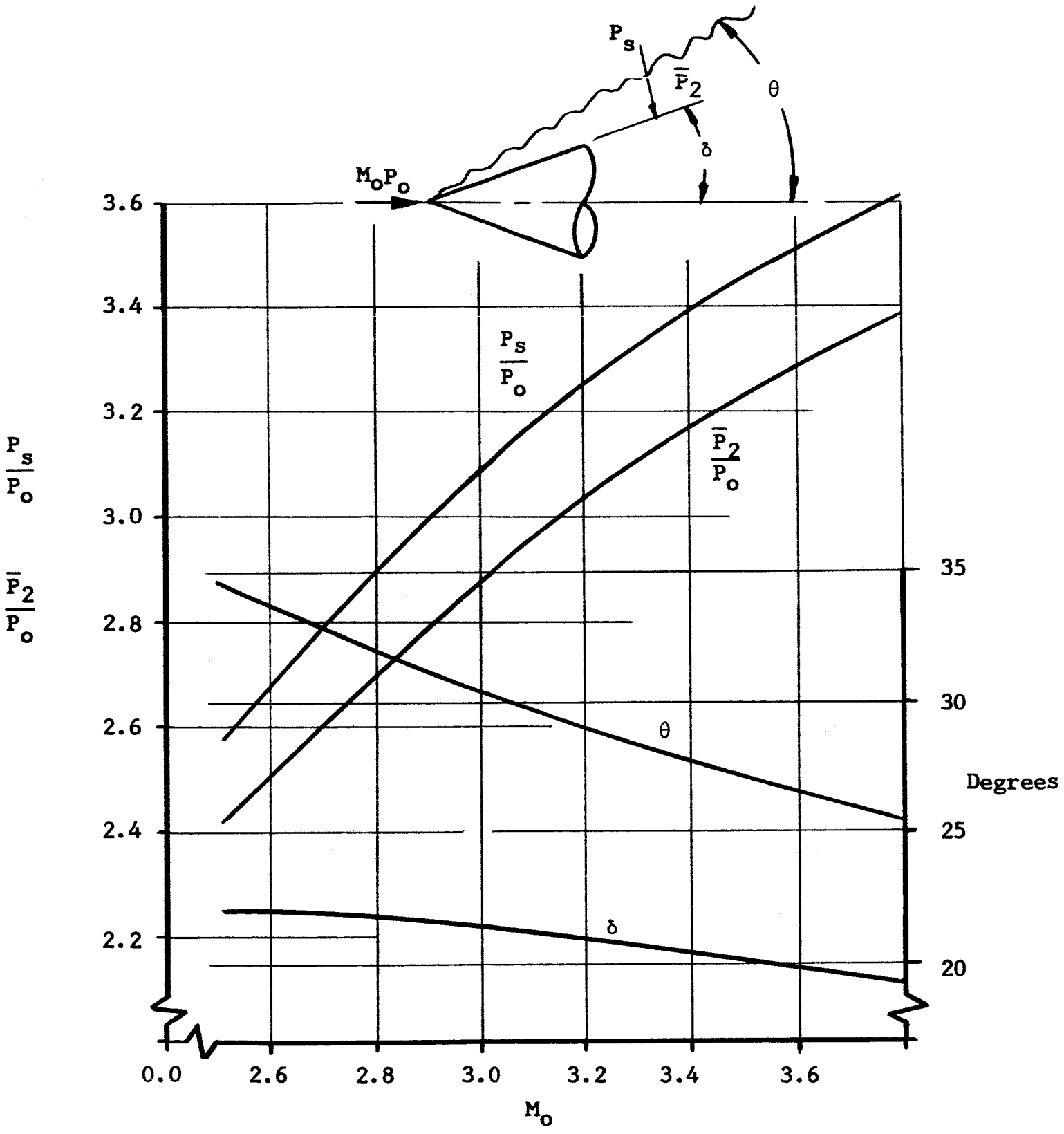

FIGURE 2.a PRESSURE RATIO OF TURBULENT BOUNDARY LAYER SEPARATED BY CONICAL SHOCK, $\gamma = 1.3$

$$A_3 = \frac{w}{P_3 M_3 \left[\frac{\gamma g}{RT_o}\left(1 + \frac{\gamma-1}{2} M_3^2\right)\right]^{1/2}}$$

(See Figure 4.a)

6) Set $\bar{P}_s = P_s = P_j = P_{t_4}$

7) Calculate M_4

$$M_4 = \left\{ \frac{2}{\gamma-1}\left[\left(\frac{P_{t_4}}{P_4}\right)^{\frac{\gamma-1}{\gamma}} - 1\right] \right\}^{1/2}$$

8) Calculate $A_{4_{total}}$ (Independent of number of injectors)

$$A_{4_{total}} = \frac{w_j \text{ total}}{P_4 M_4 \left[\frac{(\gamma g)}{RT_o}\left(1 + \frac{\gamma-1}{2} M_4^2\right)\right]^{1/2}}$$

9) $A_{exit} = A_3 + A_{4_{total}}$

10) Divide A_4 total by the X number of injectors desired to determine the contribution of one injector to the area of the primary nozzle.

11) The flow is assumed to take a hemi-cylindrical shape and the accomodation height h can be solved from geometry,

$$h = \left[\frac{2 \; A4_{total}}{X \; \pi}\right]^{1/2}$$

12) Determine the total length of the nozzle,

$$L_t = \frac{D_e - D^*}{2 \tan \alpha}$$

13) Determine the length from the exit to the location of the shock apex,

$$L_s = \frac{D_e - D_o}{2 \tan \alpha}$$

14) The distance from the apex of the shock to the center of the injection port (perpendicular injection) depends on the separation angle and the accomodation height:

$$L_x = h \, (\cot \delta + \tan \alpha)$$

15) The distance from the exit to the location of the injection port L_j can be determined from the geometrical relationship,

$$L_j = L_s - L_x \cos \alpha$$

16) The relative placement of the injector within the nozzle can be determined from,

$$\frac{L_j}{L_t} \times 100\% = \text{percentage of total length for location of injector}$$

17) The area ratio of the primary nozzle can be determined from,

$$\frac{A_e}{A^*} = \frac{A_3 + A_4}{A^*}$$

A curve can then be plotted of the area ratio and the relative placement of the injector against M_o. For the range of values of M_o = 2.6 - 3.2 with 4 injectors and the conditions given in Table 1.a, the resulting curves are presented in Figure 3.a. A position L_j/L_t = 0.25 was specified as a design condition and the corresponding area ratio and M_o were determined to be 37.5:1 and 2.95, respectively. $A_{4_{total}}$ variation with M_o was also plotted on this curve and the value of $A_{4_{total}}$ corresponding to M_o = 2.95 is 1.825 sq. in.

The throat area of the injector nozzles can be found from,

$$A^* = \frac{w_j \text{ (one injector)}}{P_o\left[\frac{\gamma g}{RT_o}\left(\frac{2}{\gamma+1}\right)^{\frac{\gamma+1}{\gamma-1}}\right]^{1/2}}$$

the choked flow equation. For the four injector design the throat area of each secondary injector is 0.01773 sq. in.

The dimensions of the 37.5:1 altitude nozzle and the relative position of the injection nozzles appear in Figure 4.a. The exit conditions of the injection nozzles are determined as,

$M_j = 2.28$

$A_j = 0.04151$ sq. in.

$P_j = 82.4$ psia

FIGURE 3.a RESULTANT AREA RATIO AND INJECTOR PLACEMENT VARIATION WITH UPSTREAM MACH NUMBER

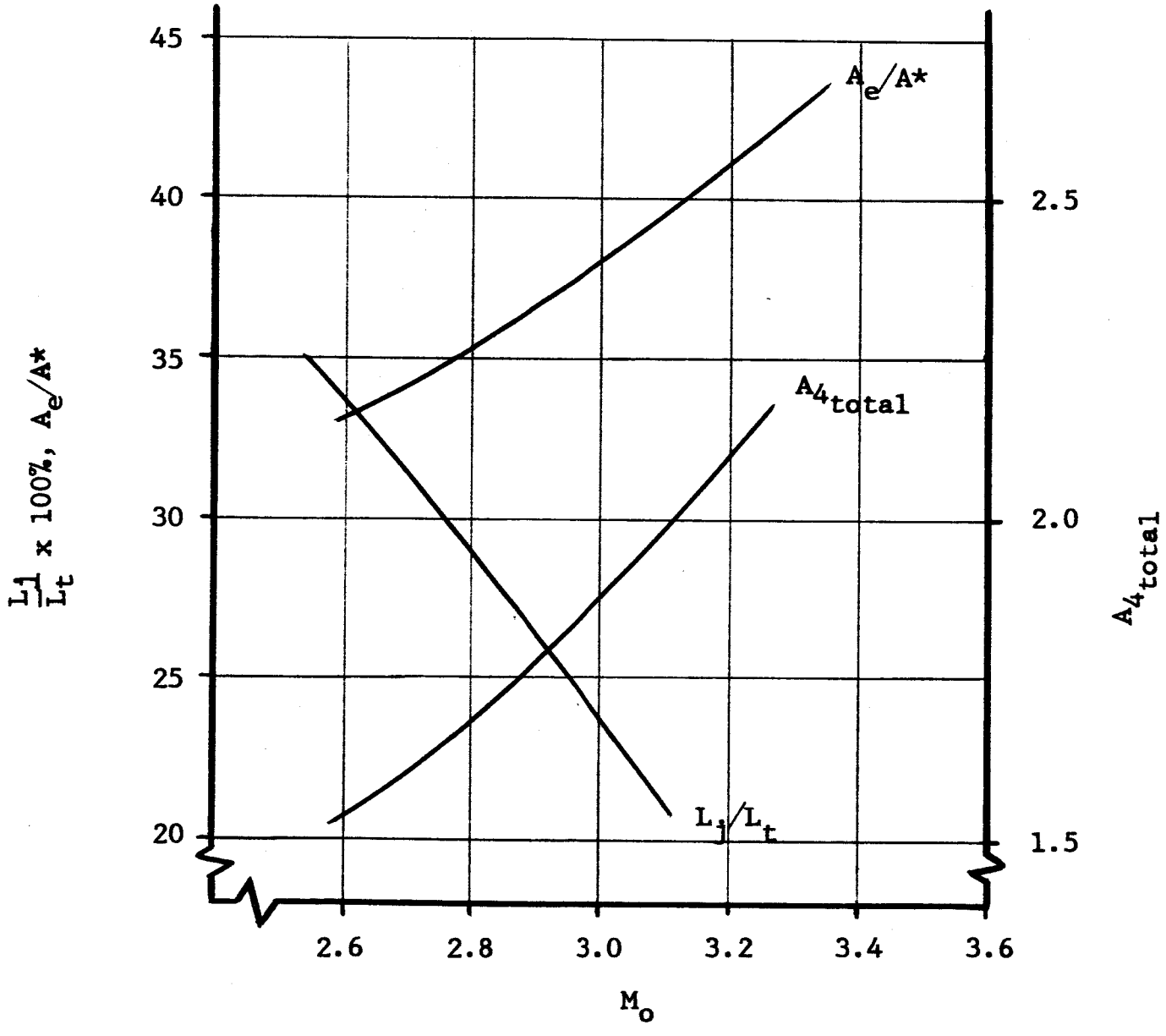

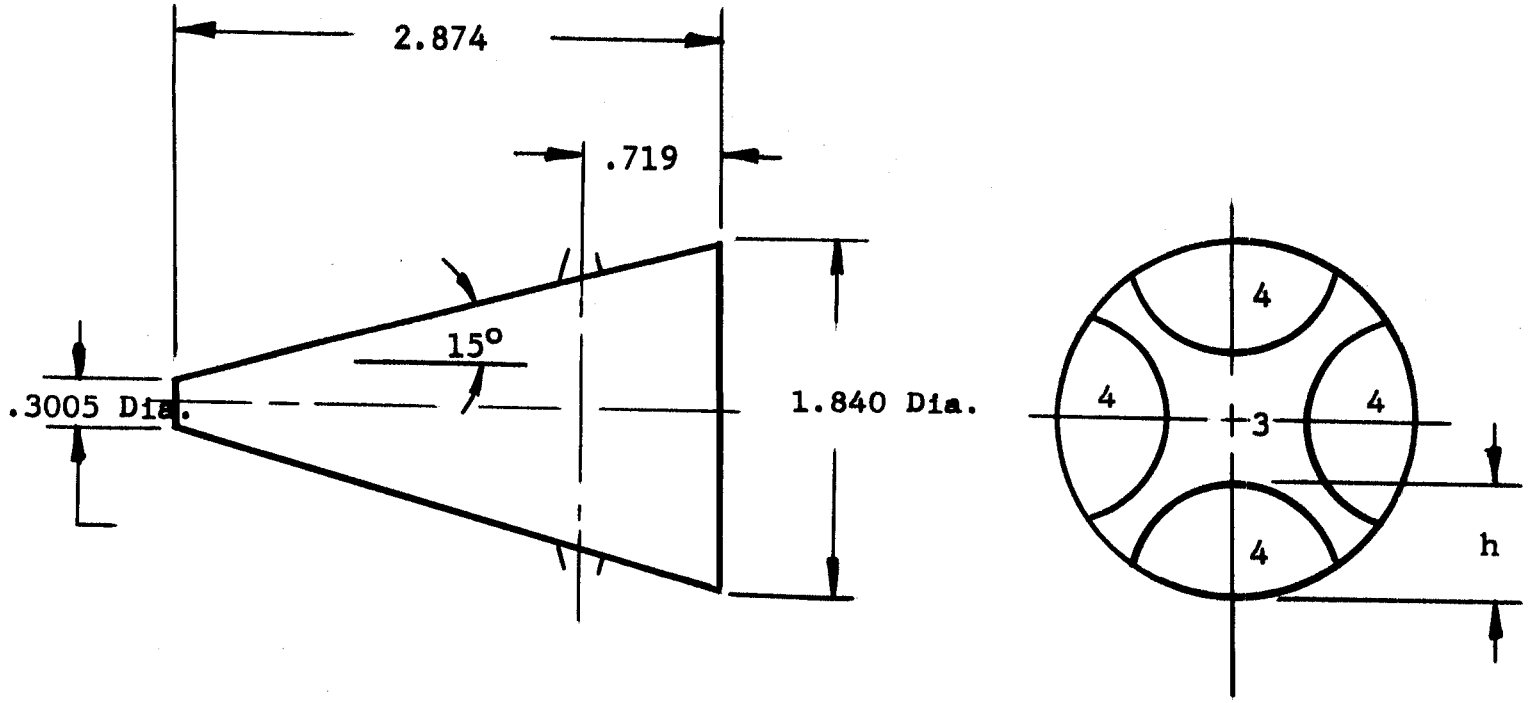

FIGURE 4.a 37.5:1 AREA RATIO NOZZLE WITH INJECTOR PLACEMENT (4 INJECTORS)

APPENDIX B

ANALYTICAL MODEL

TEST NO. 2 - 6 INJECTION PORTS WITH MODULATED INJECTED FLOW

The calculation procedure used to determine the shock location within the nozzle was the same as that presented in Appendix A with the added modification presented at the end of Section 3.2.3, for the actual to theoretical ratio of the shock location. Table 1.b presents the design parameters for the primary nozzle and secondary injection system based on the results of the test firing.

TABLE 1.b SYSTEM PARAMETERS

	Primary Nozzle	Injection System
Weight Flow (lb/sec), w	0.565	0.565
Nozzle Chamber Pressure (psia), P_c	1005	930-1000
Chamber Temperature (°R), T_c	2370	2240
Gas Constant, $\frac{ft.lb.}{lb.m°R}$, R	80.3	80.3
Ratio of Specific Heats, γ	1.279	1.279
Nozzle Half Cone Angle (degrees), α	15	15
Throat Area (in^2), A*	0.070925	.0656 (Total)

Curves of area ratio and relative placement of the injectors for a range of M_0 = 2.6-3.2 with 6 injectors are presented in Figure 1.b.

The design position for the injectors was taken as $L_j/L_t = 0.395$ with corresponding values of $A_e/A^* = 37.5:1$; $M_o = 3.12$ and $A_{4_{total}} = 1.850\ in^2$.

Also plotted on this figure is a revised value of L_j/L_t for four injectors for $h_j = .72\ h_e$.

The dimensions of the 37.5:1 altitude nozzle and the relative position of the injection nozzles appear in Figure 2.b. The exit conditions of the injection nozzles are determined as nominally:

$$M_j = 2.455$$

$$A_j = 0.031731 \text{ sq. in.}$$

$$P_j = 59.2 \text{ psia}$$

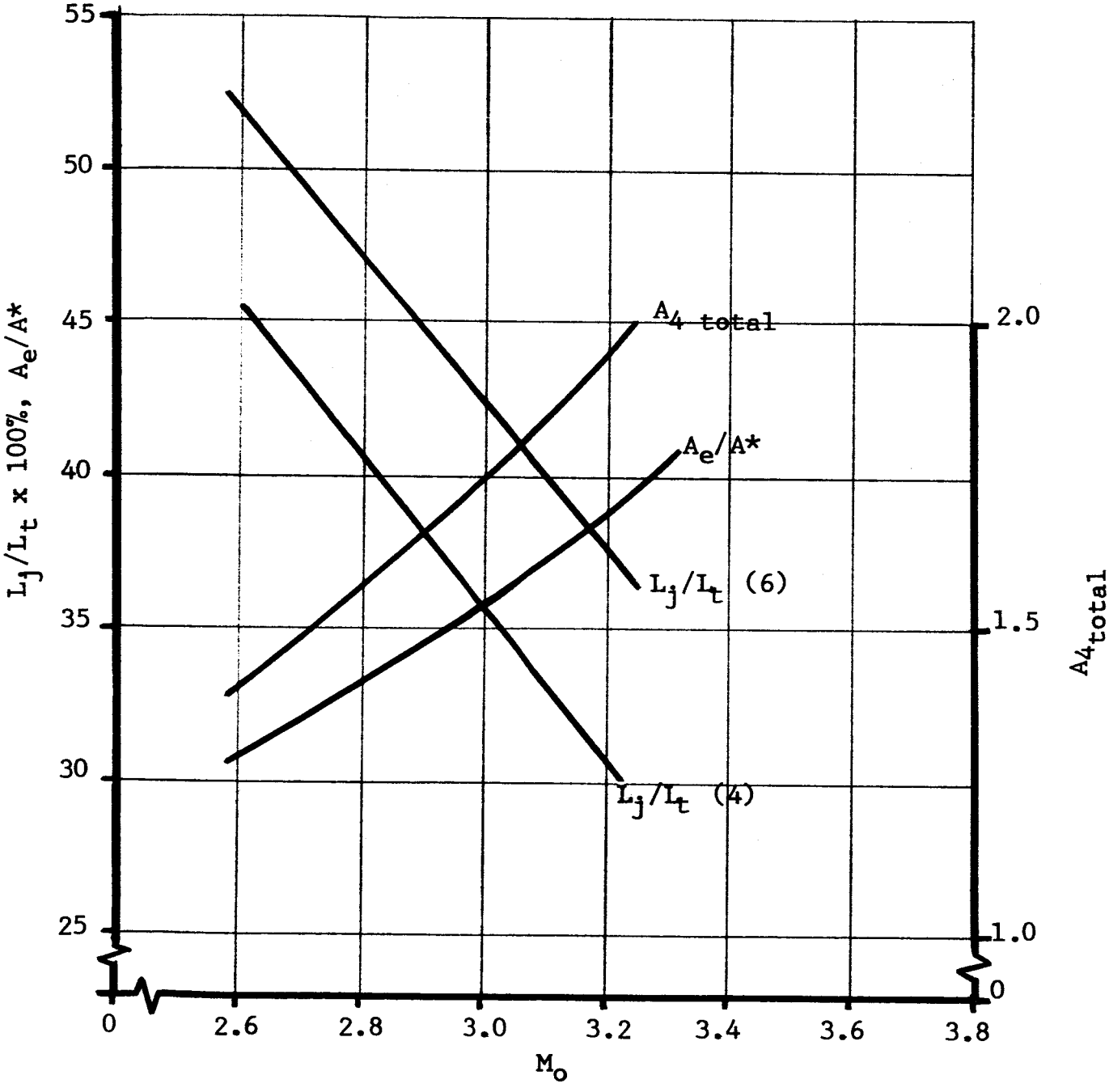

FIGURE 1.b

RESULTANT AREA RATIO AND INJECTOR PLACEMENT VARIATION WITH UPSTREAM MACH NUMBER

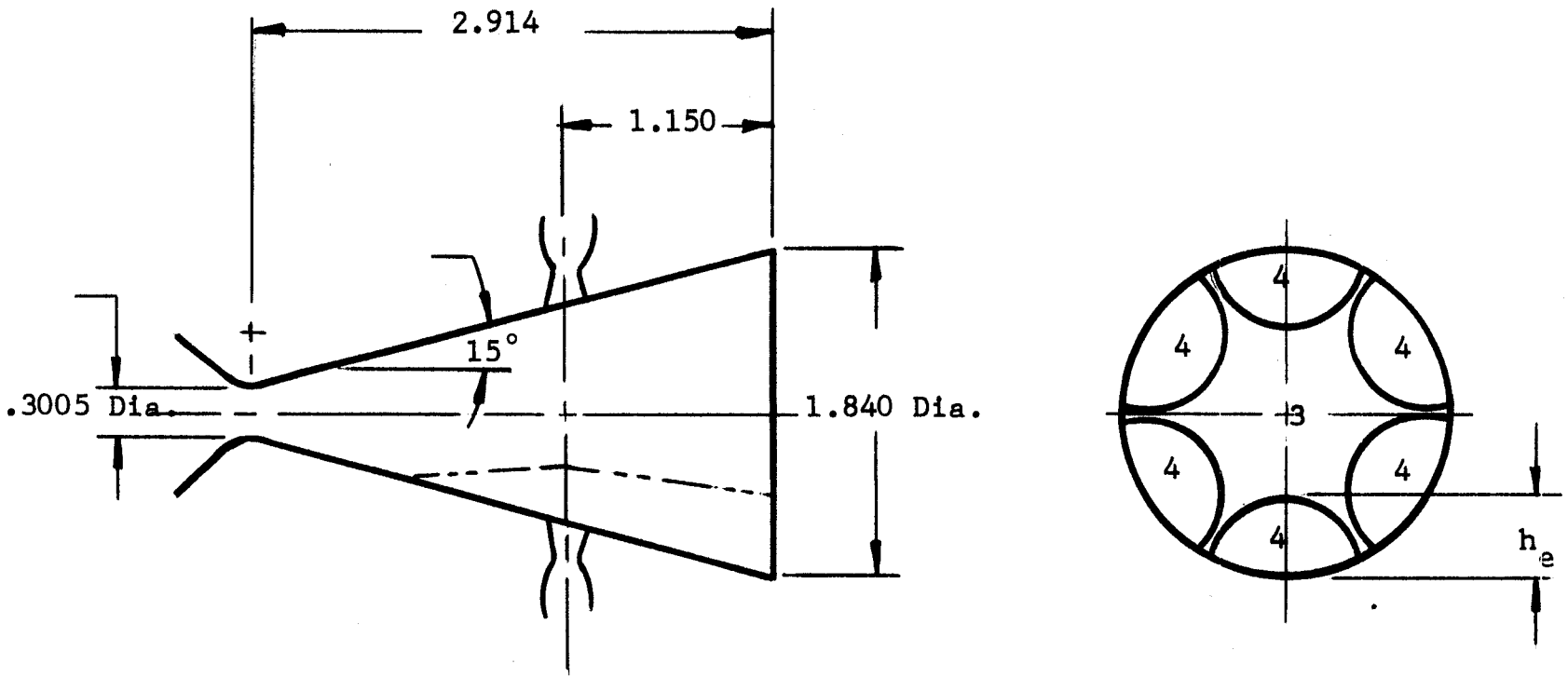

FIGURE 2.b

37.5:1 AREA RATIO NOZZLE WITH
INJECTOR PLACEMENT (6 INJECTORS)

REFERENCES

1. Vickers Proposal TP-1-29A, May 26, 1964.

2. Wu, J. M., Chapkis, R. L., and Mager, A., "Approximate Analysis of Thrust Vector Control by Fluid Injection", ARS Journal, December, 1961, pp. 1677-1685.

3. Lee, J. P., Rini, J. A., and Royston, D. L., "Theoretical Analysis of Thrust Vector Control by Gaseous Secondary Injection", TR-3-18, Vickers Incorporated, February, 1964.

4. Mager, A., "On the Model of the Free, Shock-Separated, Turbulent Boundary Layer", Journal of Aeronautical Science, February, 1956, Volume 23, pp. 181-184.

5. Shapiro, A. H., "The Dynamics and Thermodynamics of Compressible Fluid Flow", Volumes I and II, The Ronald Press Company, New York, 1953.

6. Koelle, Heing Hi, "Handbook of Astronautical Engineering", McGraw-Hill Book Company, Incorporated, New York, 1961.

7. Reinke, R. F., and Ellis, G. O., "Design of an Altitude Nozzle Compensated by Gaseous Secondary Injection", TR-5-26, Vickers Incorporated, September, 1964.